Chemical Engineering Journal 460 (2023) 141753

Contents lists available at ScienceDirect

Chemical Engineering Journal

journal homepage: www.elsevier.com/locate/cej

# Microalgal cultivation on digestate: Process efficiency and economics

S. Rossi [a,*], M. Mantovani [b], F. Marazzi [b], M. Bellucci [a,c], F. Casagli [a,d], V. Mezzanotte [b], E. Ficara [a]

[a] Politecnico di Milano, Department of Civil and Environmental Engineering (DICA), P.zza L. da Vinci 32, 20133 Milano, Italy
[b] Università degli Studi di Milano-Bicocca, Department of Earth and Environmental Sciences (DISAT), P.zza della Scienza 1, 20126 Milano, Italy
[c] Agenzia Spaziale Italiana (ASI), Via Vitaliano Brancati 48, 00144 Roma, Italy
[d] Institut National de Recherche en Informatique et en Automatique (INRIA), Biocore, Université Côte d'Azur, Route des Lucioles 2004 – BP 93, 06902 Sophia-Antipolis, France

ARTICLE INFO

*Keywords:*
Sustainable wastewater treatment
Microalgae
Digestate valorisation
Nutrient removal and recovery
Techno-economic assessment
Scenario analysis

ABSTRACT

This study aims at evaluating the process efficiency of an outdoor pilot-scale microalgae-based wastewater treatment system. Experimental results from two monitoring campaigns were analysed, showing that the system removed on average 85.1 % and 36.2 % of the influent ammoniacal nitrogen and orthophosphate, respectively, with an associated algal productivity of 9.5 g TSS·m$^{-2}$·d$^{-1}$. Based on pilot-scale results, a comprehensive techno-economic assessment was performed, allowing to calculate a biomass production cost of 4.3 €·kg TSS$^{-1}$ and a wastewater treatment cost of 2.7 €·m$^{-3}$ (corresponding to a nitrogen removal cost of 12.5 €·kg N$^{-1}$). These costs turned out to be comparable with conventional wastewater treatment processes, thus recognizing the potential of microalgae cultivation on wastewaters as feasible alternative to conventional energy-demanding bioremediation systems and to expensive algal cultivation processes. A sensitivity and scenario analysis indicated that, under the most optimistic condition (20 % increase in the productivity, and 20 % OPEX and CAPEX reduction), biomass production and nitrogen removal costs could be further reduced of approximately 44 %.

## 1. Introduction

Wastewater treatment processes are of primary importance to allow for water reuse, combined with energy and resource recovery. These processes have been studied for more than a century, and the most widely used technology is nowadays the biological treatment based on the activated sludge process (ASP). This process achieves high removal efficiencies for wastewater macro pollutants (i.e., N, P and C compounds), but has strong environmental impacts, in terms of greenhouse gas emissions [1]. In addition, the ASP uses considerable amounts of energy since oxygen must be provided to aerobic bacteria for the oxidation of ammoniacal nitrogen and organic matter. Indeed, aeration in wastewater treatment plants is the major responsible for energy consumption [2]. Different solutions have been evaluated in the last decades, trying to find more suitable and environmentally-friendly processes [3]. Within this framework, microalgae-based wastewater treatment (MBWWT) processes can strongly reduce the $CO_2$ emissions and the energy requirement for water processing [4]. Indeed, microalgae and other phototrophic microorganisms can be exploited to remove nutrients using sunlight, directly producing $O_2$ for the biological treatment units and reducing the demand of external oxygenation [5,6]. Microalgae-bacteria consortia that develop in MBWWT are typically composed by different microalgae strains, and by nitrifying and heterotrophic bacteria. The algal-bacterial biomass that is generated in the process is suitable for several valorisation alternatives, including energy recovery as biogas or biodiesel, and nutrient recovery through the production of biofertilizers and biostimulants [4,7]. Microalgae can play a major role in a global bio-economy [8], but the production costs are generally high, dictated by the cost of synthetic nutrient media and of the installation and operation of closed photobioreactors (PBRs). Such high costs can practically make the process unfeasible, unless high-value compounds are produced [9]. On the other hand, using wastewater nutrients for growing microalgae in open ponds holds a remarkable potential to cut the production costs [10]. Among the wastewater streams that are available for microalgae cultivation, municipal and agro-industrial wastewaters can be effectively used, making both microalgae cultivation and wastewater treatment attractive [11,12]. The liquid fraction of the digestate that is generated by the anaerobic digestion of waste sludge in wastewater treatment plants or by animal manure in agricultural biogas plants is an interesting substrate for microalgae cultivation, as it can provide all the required nutrients for microalgae growth [13,14]. However, the technical and economic

* Corresponding author.
*E-mail address:* simone.rossi@polimi.it (S. Rossi).

https://doi.org/10.1016/j.cej.2023.141753
Received 6 October 2022; Received in revised form 9 January 2023; Accepted 4 February 2023
Available online 6 February 2023

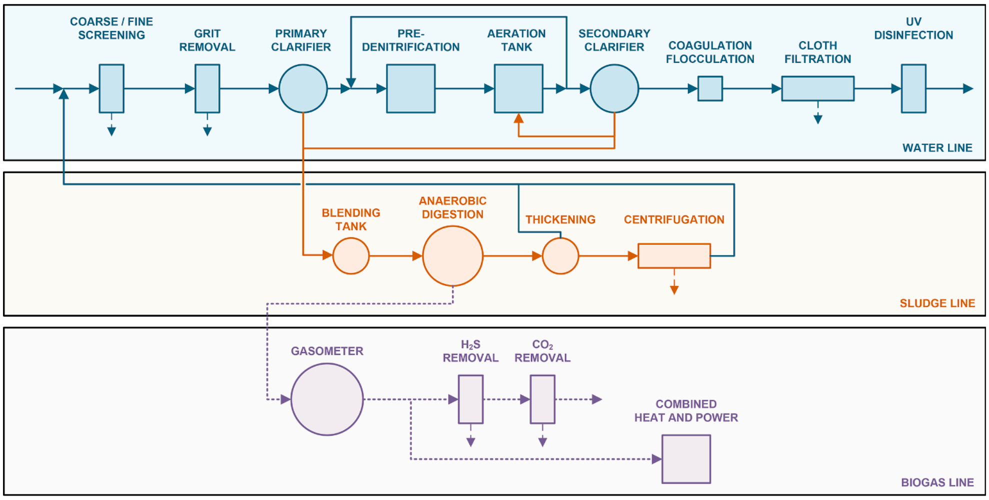


**Fig. 1.** Layout of the Bresso-Seveso WWTP.

**Table 1**
Characterisation of the digestate used to feed the microalgae cultivation unit.

| PARAMETER | UNIT | YEAR 2020 | YEAR 2021 | AVERAGE |
|---|---|---|---|---|
| TAN | mg N·L$^{-1}$ | 221 ± 29 | 183 ± 19 | 220 ± 45 |
| $NO_2^-$ | mg N·L$^{-1}$ | 0.2 ± 0.2 | 0.4 ± 0.3 | 0.3 ± 0.2 |
| $NO_3^-$ | mg N·L$^{-1}$ | 0.6 ± 0.2 | 0.1 ± 0.0 | 0.4 ± 0.6 |
| TN | mg N·L$^{-1}$ | 222 ± 3 | 184 ± 19 | 221 ± 45 |
| $PO_4^{3-}$ | mg P·L$^{-1}$ | 8.1 ± 1.5 | 10.9 ± 1.4 | 8.9 ± 2.2 |
| TP | mg P·L$^{-1}$ | 10.1 ± 1.6 | 13.1 ± 1.1 | 11.5 ± 2.0 |
| $COD_S$ | mg COD·L$^{-1}$ | 122 ± 34 | 213 ± 55 | 151 ± 57 |
| $COD_{TOT}$ | mg COD·L$^{-1}$ | 290 ± 91 | 301 ± 40 | 296 ± 70 |
| ALK/TAN | mol·mol $^{-1}$ | 1.24 ± 0.25 | 1.57 ± 0.28 | 1.50 ± 0.30 |
| $OD_{680}$ | – | 0.15 ± 0.10 | 0.12 ± 0.06 | 0.12 ± 0.07 |
| TSS | g TSS·L$^{-1}$ | 0.23 ± 0.11 | 0.25 ± 0.09 | 0.22 ± 0.10 |
| VSS | g VSS·L$^{-1}$ | 0.15 ± 0.04 | 0.18 ± 0.05 | 0.16 ± 0.05 |
| Turbidity | FAU | 160 ± 92 | 90 ± 42 | 103 ± 76 |
| pH | – | 8.3 ± 0.3 | 8.6 ± 0.2 | 8.5 ± 0.3 |

feasibility of using digestate for producing microalgae at the industrial scale has not been demonstrated and quantified in available literature reports. This work aims at evaluating the process efficiency of a microalgae-based system for digestate treatment operating at middle-low latitudes, through the assessment of nutrient removal capabilities and biomass productivities at the pilot-scale. Based on the results obtained from two experimental campaigns, a comprehensive techno-economic assessment was performed, including all relevant cost items for the process. Thus, this study provides a realistic evaluation of the algal production cost at the full-scale by using recycled nutrients from the waste stream.

## 2. Materials and methods

### 2.1. Wastewater treatment plant and wastewater characteristics

#### 2.1.1. Wastewater treatment plant

The pilot-scale experimentation was conducted inside a wastewater treatment plant (WWTP) located in Milan, Italy (Latitude: 45°31′31.915″N, Longitude: 9°11′42.997″E), treating wastewater from 220,000 population equivalents (P.E.). The WWTP is composed by conventional water and sludge treatment lines. The water line includes: mechanical preliminary treatments (coarse and fine screening; sand, grit, and oil removal), primary treatment (settling), secondary treatments (denitrification/nitrification) and tertiary treatments (filtration and UV disinfection). The sludge line includes: anaerobic digestion (mesophilic digestion of mixed primary/secondary sludge), post-thickening, and sludge dewatering (polyelectrolyte-assisted centrifugation). A dedicated biogas line is also present, where the biogas from anaerobic digestion is first stored in a gasometer and then either utilized in a combined heat and power (CHP) unit to cover part of the plant auto-consumption or upgraded to biomethane (desulphurization and hollow-fibre membrane filtration) for injection into the national gas grid; the $CO_2$ from biogas upgrading is available for microalgae cultivation on digestate. A schematic representation of the Bresso-Seveso WWTP is provided in Fig. 1.

#### 2.1.2. Digestate characteristics

The liquid fraction of the digestate (hereafter simply referred to as "digestate") was used to feed the pilot-scale microalgae-bacteria cultivation unit. The digestate has suitable characteristics as microalgae growth medium (Table 1), due to the low content of suspended solids (resulting in a low turbidity and optical density), and the relatively low concentrations of Total Ammoniacal Nitrogen (TAN), as previously reported [13,15]. However, the concentration of total alkalinity (ALK) is low in the digestate, resulting in an ALK to TAN ratio that could make the inorganic carbon concentration limiting for the growth of microalgae and nitrifying bacteria [16]. Therefore, the digestate was supplemented with sodium bicarbonate.

### 2.2. Pilot-scale experimentation

#### 2.2.1. Microalgae cultivation unit

Microalgae cultivation was performed in a pilot-scale raceway pond (RWP) provided by SEAM Engineering S.r.l. and described in a previous work [15]. The RWP had a total surface of 5.8 m$^2$ with an adjustable gravity overflow drain set to 0.13 – 0.15 m, resulting in an overall volume of 0.75 – 0.87 m$^3$. A paddlewheel with an adjustable revolution speed was used for mixing the algal suspension, being constantly operated at 4 RPM. The area covered by the paddlewheel was approximately 1.5 m$^2$, so that the effective surface receiving the solar radiation is approximately 4.3 m$^2$ which was the surface used for calculating the areal biomass productivity. The RWP was covered by a greenhouse, protecting the culture from heavy rain events, and increasing the temperature during the wintertime. During spring, summer, and autumn, the lateral openings of the greenhouse were removed to prevent excessive temperatures. The influent digestate was stored in a container (1 m$^3$ volume) and fed to the RWP by a peristaltic pump. The RWP was sparged from the bottom with $CO_2$ (either a pure $CO_2$ cylinder, or to the reject $CO_2$ line from biogas upgrading) via a temporized electro-valve operating for 2 – 8 min·d$^{-1}$ with flowrates of 1.0 – 1.5 Nm$^3$·h$^{-1}$. The pond was equipped with a PLC, and with online probes for: temperature, Dissolved Oxygen (DO) concentration, pH, turbidity, TAN and $NO_X$

**Table 2**
Main operational conditions of the raceway pond during the two monitoring campaigns.

| PARAMETER | UNIT | MONITORING CAMPAIGN YEAR 2020 | YEAR 2021 |
|---|---|---|---|
| Duration | d | 103 | 210 |
| Period | – | July – October | May – December |
| HRT | d | 8.6 – 10 | 6 |
| Liquid height | m | 0.13 – 0.15 | 0.15 |
| $CO_2$ source | – | Pure $CO_2$ | $CO_2$ from biogas upgrading |
| Corrected ALK/TAN ratio | – | 1.20 – 1.73 | 1.95 – 2.60 |
| pH of the suspension | – | 5.8 – 8.2 | 7.0 – 8.2 |
| Average daily pond temperature | °C | 11.2 – 26.9 | 20.8 – 29.6 |
| Pond thermal excursion | °C | 1.0 – 13.3 | 0.6 – 9.3 |
| Average daily irradiance | $\mu E \cdot m^{-2} \cdot s^{-1}$ | 217 – 695 | 400 – 737 |

concentrations, and solar radiation.

### 2.2.2. Monitoring campaigns and operational conditions

The RWP was operated in two consecutive years (2020 and 2021), during periods typically characterized by favourable weather conditions for algal growth at these latitudes. The monitoring campaign of 2020 lasted for 103 days (from July to October), due to the limitations imposed by the COVID-19 pandemics, while in 2021 the pilot RWP was fully operative, and it was monitored for 210 days (from May to December). In both cases, the RWP was inoculated with a mixed microalgae-bacteria consortium, containing mainly *Chlorella*, *Scenedesmus*, and *Chlamydomonas* spp., and acclimated in batch conditions for two weeks with diluted digestate (1:2). Then the system was switched to the continuous feeding operation mode, with an HRT of 8.6 – 10 days in 2020 and of 6.0 days in 2021. The HRTs were calculated based on the influent digestate flowrate and the reactor volume ($HRT = V \cdot Q_{IN}^{-1}$). Pure $CO_2$ was bubbled in the 2020 campaign, while the reject $CO_2$ stream from biogas upgrading was used during 2021. The liquid discharge was conducted manually during 2020, resulting in a varying liquid height (from 0.13 to 0.15 m), while continuous outflow was allowed in 2021, when the RWP was operated at the liquid height of 0.15 m. The lateral coverage of the greenhouse was only mounted during December 2021. In both campaigns, the ALK to TAN ratio was modified by dosing $NaHCO_3$, until reaching average values of 1.3 ± 0.2 in the 2020 campaign, and 2.1 ± 0.5 in the 2021 campaign. During 2021, the ALK to TAN ratio was increased compared to the previous year, to further increase inorganic carbon availability and sustain autotrophic (microalgae and nitrifying bacteria) growth, according to previous studies [16]. Table 2 summarizes the main operational conditions for the two monitoring campaigns.

Measured weather data were retrieved from the database of the regional agency for environmental protection, ARPA Lombardia (https://www.arpalombardia.it). The weather station is located 2 km away from the microalgae cultivation unit. The main environmental conditions (i.e., air temperature and irradiance) for the two monitoring campaigns are reported in Fig. 2. To convert the solar radiation data into the desired units, a conversion factor of 2.105 $\mu E \cdot m^{-2} \cdot s^{-1} \cdot (W \cdot m^{-2})^{-1}$ was used, following Sulev & Ross [17] and coherently with previous works [18]. Weather data showed no statistical difference among the two monitoring campaigns (at the level of significance of 95 %), suggesting that the observed differences among the two campaigns are related to the process operation, rather than to environmental conditions.

### 2.2.3. Sampling and analytical methods

To properly characterize the dynamics of the algal suspension and the influent digestate, the following parameters were routinely analysed (every 5 – 9 days): pH, concentrations of nutrients and solids, optical properties, and physico-chemical characteristics. Nutrient analyses included: Total Ammoniacal Nitrogen ($TAN = N\text{-}NH_4^+ + N\text{-}NH_3$), oxidized nitrogen forms ($N\text{-}NO_2^-$ and $N\text{-}NO_3^-$) orthophosphate ($P\text{-}PO_4^{3-}$), total P ($P_{TOT}$), soluble and total COD ($COD_S$ and $COD_{TOT}$). Optical

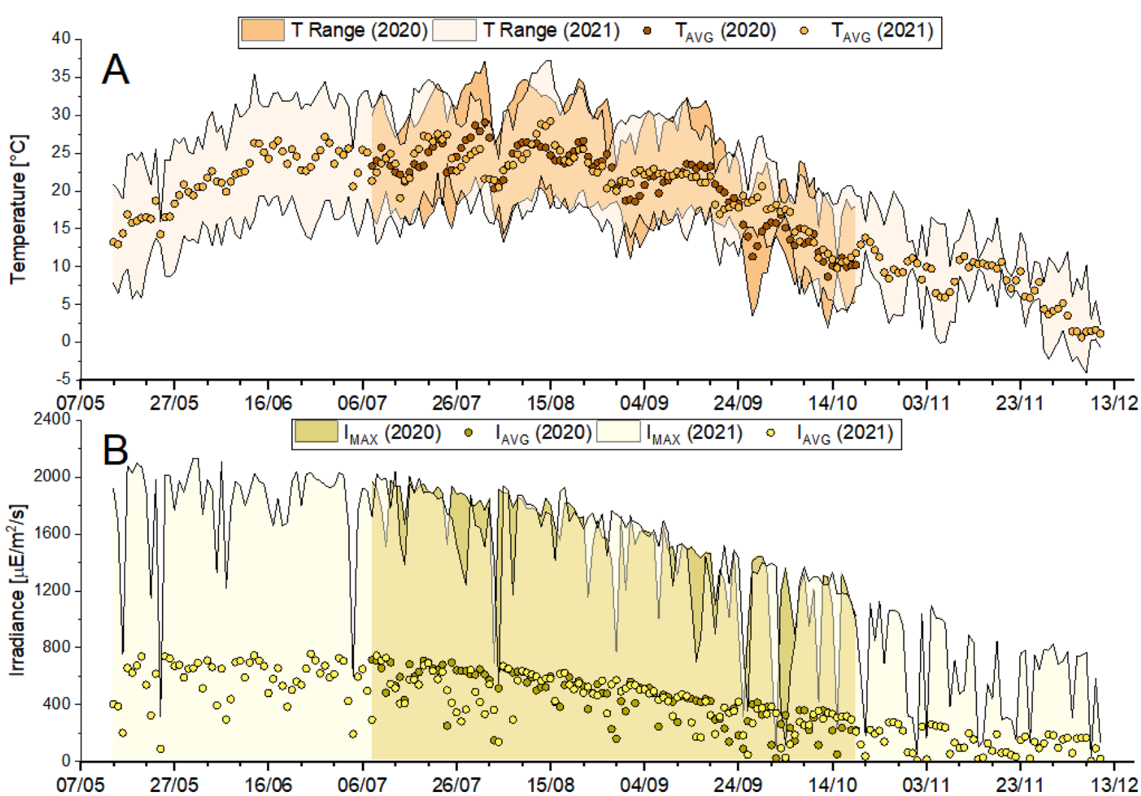


**Fig. 2.** Average daily air temperature (A) and irradiance (B) measured during the two monitoring campaigns.

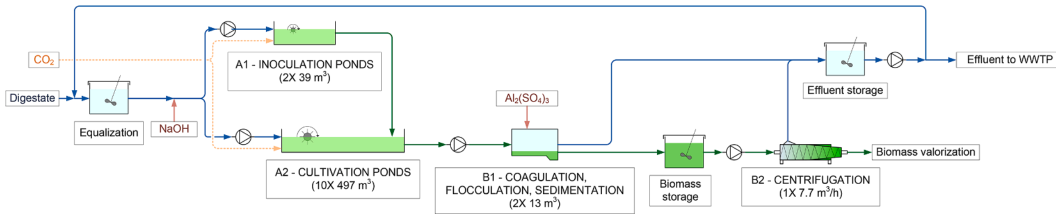


**Fig. 3.** Layout of the proposed microalgae cultivation plant.

characterization included turbidity and optical density at the wavelength of 680 nm ($OD_{680}$). The physical–chemical properties analysed were pH, temperature, and electric conductivity. The growth of microalgae was monitored by algal counts and by the concentration of Total Suspended Solids (TSS) and Volatile Suspended Solids (VSS).

As for the analytical methods, soluble nutrients, i.e., TAN, N-$NO_2^-$, N-$NO_3^-$, P-$PO_4^{3-}$, and $COD_S$ were measured on membrane-filtered samples (cut-off: 0.45 μm), using commercial test kits (Hach Lange, test codes: LCK303, LCK342, LCK339, LCK348, and LCK314, respectively). Compounds to be measured in the particulate phase, including $P_{TOT}$ and $COD_{TOT}$ were measured on unfiltered samples after digestion (1 h at 100 °C and 2 h at 148 °C, respectively) in a thermostat, using the same test kits as for soluble compounds. Test kits were then read spectrophotometrically. The $OD_{680}$ and turbidity were measured using the same instrument, in plastic cuvettes with light paths of 1 and 5 cm, respectively. Cell counts were determined using a Bürker chamber with 0.04 $mm^2$ squares, under a light microscope at 40X magnification. The microalgal species were contextually identified by visual examination. TSS and VSS were determined according to the Standard Methods for the Examination of Water and Wastewater [19]. Temperature, pH, and electric conductivity of the samples were measured immediately after sampling, using a portable multi-meter probe. The alkalinity was monitored on both the influent digestate and outlet samples of the RWP, by potentiometric titration with $H_2SO_4$ (0.02 N), according to the Standard Methods [19].

### 2.2.4. *Calculations*

Based on laboratory analyses, mass balances were calculated for each relevant parameter, by considering the RWP as a completely mixed reactor. This assumption was justified by the small scale of the pilot reactor [14,20]. The hydraulic balance of the RWP was considered to calculate the effluent flowrate, as follows (**Equation (1)**):

$$Q_{OUT}(t_i) = Q_{IN}(t_i) - Q_{EV}(t_i) \tag{1}$$

where: $Q_{OUT}(t_i)$ is the effluent flowrate at the time step $t_i$, $Q_{IN}(t_i)$ is the influent flowrate, and $Q_{EV}(t_i)$ is the evaporation rate calculated using the Buckingham model, as detailed in Pizzera et al. [14]. In the hydraulic balance, the contribution of the rainfall was neglected, since the RWP was always covered by the greenhouse roof. Once the influent and effluent flowrates were calculated, the rates of production or consumption for a generic soluble or particulate element (identified as X) could be evaluated (**Equation (2)**).

$$R_X(t_i) = \frac{\Delta X}{\Delta t} - \frac{Q_{AVG,IN}(t_i)\cdot X_{AVG,IN}(t_i)}{V_{AVG}(t_i)} + \frac{Q_{AVG,OUT}(t_i)\cdot X_{AVG,OUT}(t_i)}{V_{AVG}(t_i)} + \frac{X_{AVG,OUT}(t_i)}{V_{AVG}(t_i)}\cdot\frac{\Delta V}{\Delta t} \tag{2}$$

where: $R_X(t_i)$ [g X·m$^{-3}$·d$^{-1}$] is the transformation rate for the element X at the time $t_i$, $\Delta X = (X_i - X_{i-1})$ [g X·m$^{-3}$] is the variation in the concentration of the element X in the time interval; $\Delta t = (t_i - t_{i-1})$ [d], $Q_{AVG,IN}(t_i)$ and $Q_{AVG,OUT}(t_i)$ [m$^{-3}$·d$^{-1}$] are the average values of the influent and effluent flowrates along the time interval, respectively, $X_{AVG,IN}(t_i)$ and $X_{AVG,OUT}(t_i)$ [g X·m$^{-3}$] are the average values of the influent and effluent concentrations of X in the time interval, respectively, and $V_{AVG}(t_i)$ [m$^3$] is the average value of the volume.

In case the RWP volume is constant, **Equation (2)**, simplifies to **Equation (3)**:

$$R_X(t_i) = \frac{\Delta X}{\Delta t} - \frac{Q_{AVG,IN}(t_i)\cdot X_{AVG,IN}(t_i)}{V} + \frac{Q_{AVG,OUT}(t_i)\cdot X_{AVG,OUT}(t_i)}{V} \tag{3}$$

In **Equation (2)** and **Equation (3)**, production rates result as positive, while removal rates have negative sign. For simplicity, when referring to a nutrient removal rate (e.g., for $R_{TAN}$ and $R_{PO4}$), the absolute value of such computation is reported. The volumetric biomass productivity ($P_V$) was considered equal to the rate of TSS production ($R_{TSS}$), in accordance with previous studies [14,15]. The areal biomass productivity ($P_A$, **Equation (4)**) was referred to the surface of the RWP, and since the paddlewheel had a large footprint, locally providing a significant shading of the culture, $P_A$ was calculated by accounting for the effective area that received the solar radiation, as previously proposed [21]:

$$P_A(t_i) = P_V(t_i)\cdot\frac{V_{AVG}(t_i)}{A^*} = R_{TSS}(t_i)\cdot\frac{V_{AVG}(t_i)}{A^*} \tag{4}$$

where: $P_A(t_i)$ [g TSS·m$^{-2}$·d$^{-1}$] is the areal biomass productivity at the time i, $P_V(t_i)$ [g TSS·m$^{-3}$·d$^{-1}$] is the volumetric biomass productivity, $A^* = (A_{RWP} - A_{PW})$ [m$^2$] is the illuminated area.

The photosynthetic efficiency was calculated according to previous studies [22], as shown in **Equation (5)**.

$$\eta_{PHO} = \frac{E_{ALG}}{E_I} = \frac{P_A\cdot LHV_{ALG}}{E_I} \tag{5}$$

where: $\eta_{PHO}$ [%] is the photosynthetic efficiency, $E_{ALG}$ [MJ·m$^{-2}$·d$^{-1}$] is the amount of energy in the algal biomass, $LHV_{ALG} = 21$ [MJ·kg DW$^{-1}$] is the lower heating value of the algal biomass, and $E_I$ [MJ·m$^{-2}$·d$^{-1}$] is the amount of energy received by the pond.

To quantify the amount of free ammonia nitrogen (FAN) produced in the system, the following relation was used [23,24], based on the actual TAN, pH and temperature measured in the RWP (**Equation (6)**).

$$FAN = \frac{TAN\cdot 10^{pH}}{10^{pH} + \exp\left(\frac{6.344}{T_P}\right)} \tag{6}$$

where: $T_P$ [K] is the temperature of the raceway pond.

### 2.2.5. *Statistical methods*

Correlations among the methods for evaluating the algal biomass and solids were assessed through Pearson's coefficients. To determine the statistical difference among weather data in the two monitoring campaigns, the paired *t*-test was run on comparable datasets (i.e., during the period in which data were available for both monitoring campaign, July – October). All analyses were performed at the significance level of 95 % (i.e., with α = 0.05), using the software OriginPro 2020b.

## 2.3. *Techno-economic assessment*

### 2.3.1. *Proposed layout for the integration of the algae-based process in the WWTP*

For the integration of algal cultivation as a side-stream digestate

**Table 3**
Main design hypothesis for the techno-economic assessment.

| SECTION | PARAMETER | UNIT | VALUE | REFERENCE / NOTES |
|---|---|---|---|---|
| GENERAL DATA | Biomass composition | – | $CH_{1.83}O_{0.48}N_{0.11}P_{0.01}$ | [20,35] |
| | N content in the algal biomass | % w/w | 6.6 | Based on biomass composition |
| | Digestate availability | $m^3 \cdot h^{-1}$ | 90 | From WWTP data |
| | N concentration in the digestate | $g \cdot m^{-3}$ | 220 | Based on pilot data |
| | Specific area requirement | $m^2 \cdot PE^{-1}$ | 0.5 | [36,37] |
| | Total algae cultivation area required | ha | 1.98 | Based on the specific area requirement |
| | Net/gross area ratio for RWPs | – | 0.8 | [29] |
| | Operativity of the plant | $d \cdot y^{-1}$ | 274 | Considering operativity from March to November |
| | Algal productivity | g $TSS \cdot m^{-2} \cdot d^{-1}$ | 9.9 | Based on pilot data and photosynthetic efficiency |
| | Increase productivity coefficient | – | 1.2 | 20 % gain due to higher irradiance without greenhouse |
| | Number of paddlewheels per RWPs | – | 1 | Assumed |
| A1 – INOCULATION PONDS | Area requirement | % | 2 | Of the total algae cultivation area |
| | Net area required | ha | 0.04 | Based on total area required |
| | Number of RWP modules | – | 2 | Based on module design |
| | Module length | m | 49 | Assumed |
| | Module width | m | 4 | Assumed |
| | Liquid height | m | 0.2 | Assumed |
| | Total volume | $m^3$ | 78.4 | Calculated |
| | Digestate treated | $m^3 \cdot d^{-1}$ | 7.5 | Based on RWPs volume and HRT |
| | Effluent biomass concentration | g $TSS \cdot m^{-3}$ | 631 | Based on treated digestate and productivity |
| A2 – CULTIVATION PONDS | Area requirement | % | 98 | On the total algae cultivation area |
| | Net area required | ha | 1.94 | Based on total area required |
| | Number of RWP modules | – | 10 | Based on module design |
| | Module length | m | 153 | Assumed |
| | Module width | m | 13 | Assumed |
| | Liquid height | m | 0.25 | Assumed |
| | Total volume | $m^3$ | 4,972 | Calculated |
| | Digestate treated | $m^3 \cdot d^{-1}$ | 365 | Based on RWPs volume and HRT |
| | Effluent biomass concentration | g $TSS \cdot m^{-3}$ | 642 | Based on treated digestate and productivity |
| | NaOH concentration required | mM NaOH | 25 | To correct influent alkalinity [16] |
| B1 – COAGULATION, FLOCCULATION, SEDIMENTATION | Flocculant added | – | $Al_2(SO_4)_3$ | Assumed |
| | Flocculant dosage | g $Al \cdot m^{-3}$ | 15 | [31] |
| | Contact time | min | 15 | Assumed |
| | HRT in the coagulation zone | h | 1.75 | [30] |
| | Solids removal efficiency | % | 95 | [31] |
| | Effluent biomass concentration | kg $TSS \cdot m^{-3}$ | 5 | [29] |
| B2 – CENTRIFUGATION | Flowrate treated | $m^3 \cdot d^{-1}$ | 46.1 | Based on productivity and pre-concentration effluent |
| | Solids removal efficiency | % | 95 | [21] |
| | Effluent biomass concentration | kg $TSS \cdot m^{-3}$ | 200 | [29] |

treatment, the algae-bacteria unit is aimed at removing nutrients (N and P) from digestate, and at utilizing the $CO_2$ available from the full-scale biogas upgrading section converting it into potentially valuable biomass. As suggested by the data retrieved at the pilot scale, it was assumed that no specific pre-treatments were required for the liquid fraction of the digestate. Therefore, the plant only includes an algae/bacteria cultivation line and a subsequent biomass concentration, to produce an algal paste for further utilization/processing. As depicted in Fig. 3, the plant layout is composed by the following sections: (A) biomass production, including inoculation ponds (section A1) and cultivation ponds (section A2); (B) biomass harvesting, including biomass pre-concentration (section B1) and harvesting through centrifugation (section B2). The proposed process produces a highly concentrated algal biomass stream and a treated digestate stream. The treated digestate is then recirculated to the head of the water line. The produced algal-bacterial paste can be valorised in a biorefinery perspective, following different valorisation pathways [25–27]. The production of low-value products, such as bioplastics or biofuels (biogas or biodiesel) is typically adopted for the wastewater-grown biomass since it is not possible to valorise it as food or feed applications. The concurrent production of bio-stimulants for the agricultural market could be considered as an interesting alternative. However, only the biomass production is analysed in this section, aimed at evaluating the costs and feasibility of scaling-up the production line, in view of a subsequent decision-making about the best valorisation alternative.

### 2.3.2. *Techno-economic assessment*

Relevant design hypotheses for each section composing the layout shown in Fig. 3 are presented below and further detailed in Table 3.

**General design data**

Section A – Biomass production

According to pilot-scale productivity and weather data for the considered location, the biomass production is calculated by considering an operativity of the plant of 9 months per year (from March to November, i.e., for 274 $d \cdot y^{-1}$). During this operational period, an average productivity of 9.9 g $TSS \cdot m^{-2} \cdot d^{-1}$ was calculated, based on the average photosynthetic efficiency reached in the pilot-scale experiments ($\eta_{PHO}$ = 1.83 %) and local irradiance data. The obtained productivity was further incremented by 20 %, since in the scaled-up process no greenhouse is foreseen, and this will lead to a higher light availability [28]. The approach of considering a 20 % increase in the productivity is still conservative, since the irradiance reduction due to the greenhouse can reach up to 40 % (according to measured PAR data, data not shown). This would also compensate the eventual contribution of rainfall events, that are not explicitly considered in this analysis. As reported in previous works [21,29], low-cost systems are used for the inoculum and

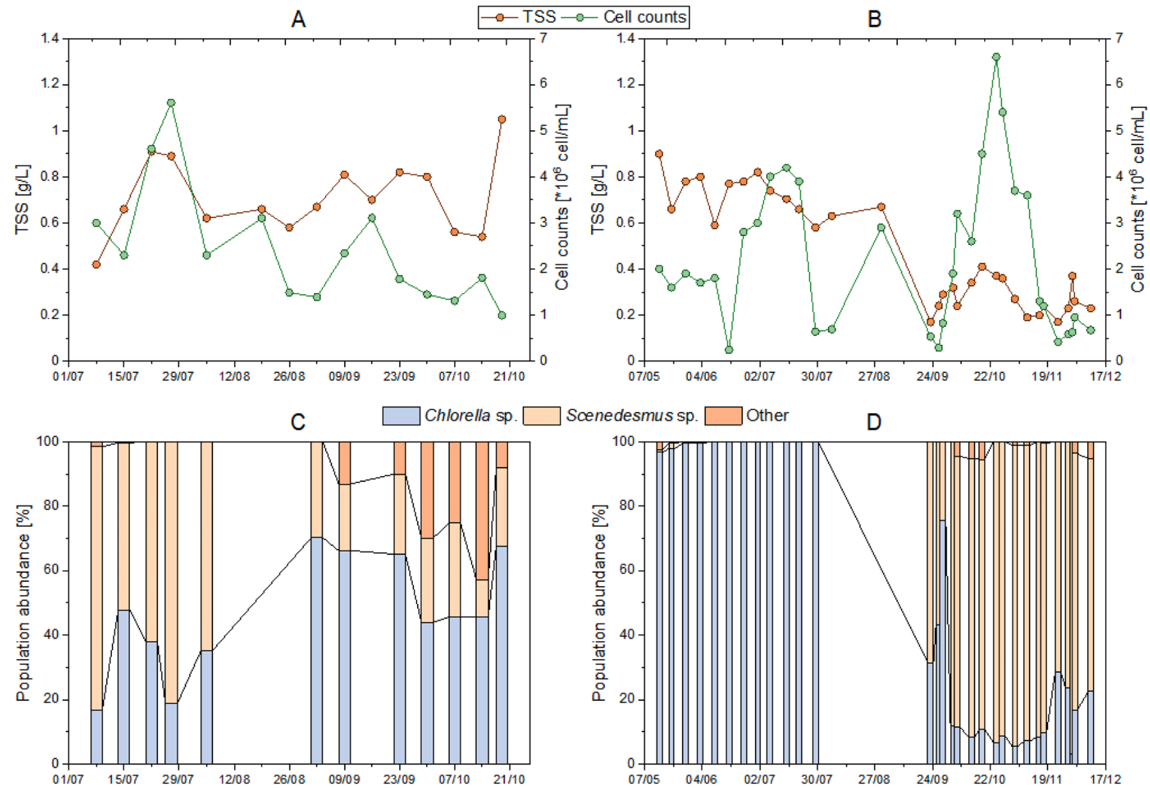


**Fig. 4.** Evolution of biomass concentration and microalgal communities: total suspended solids and microalgal cell counts for 2020 (A) and 2021 (B), microalgal population relative abundance in 2020 (C) and 2021 (D).

cultivation RWPs. The ponds are therefore constituted by a waterproof lining laid on the ground, and by concrete walls to hold the liner in place. RWPs are provided with a paddlewheel for mixing the algal suspension and with the instrumentation needed to monitor the state of the process, i.e., with DO, pH, and temperature probes connected to a PLC for remote monitoring. As for the sizing of inoculation and cultivation ponds, the required volume is calculated based on the maximum digestate availability and the imposed HRT (Table 3). The inoculum section (A1), which is aimed at guaranteeing a more rapid start-up of the plant in the event of occasional crashes, is constituted by 2 RWPs having a total length of 49 m, and a width of 4 m (total surface of 0.04 ha) and a liquid depth of 0.2 m (total volume of 78.4 $m^3$). The biomass cultivation section (A2) is constituted by 10 RWPs with length of 153 m and width of 13 m (overall pond surface of 1.94 ha), and a liquid depth of 0.25 m (volume of 4972 $m^3$). Regarding the arrangement of RWPs, a distance among ponds of 3 m was considered, to allow for maintenance operations and for placing piping and wiring. As suggested by pilot results, NaOH supplementation was considered to correct the ALK to TAN ratio of the influent digestate to 1.6 mol·$mol^{-1}$ [16]. Digestate feeding pumps (operated for 24 h·$d^{-1}$) were designed according to conventional hydraulic criteria keeping into account friction head losses, and by considering that each feeding pump would serve two RWPs.

Section B – Biomass concentration and harvesting

The biomass pre-concentration section (B1) is assumed to include two coagulation, flocculation, and sedimentation (CFS) tanks, each serving five of the RWPs of section A2. Each CFS tanks is divided into a coagulation section with fast mixing, a flocculation zone with no mixing, and a calm zone realized by lamellar settling [21,30]. Based on previous lab-scale tests [31], aluminium sulphate ($Al_2(SO_4)_3$) is dosed in the coagulation zone to reach a concentration of 15 g Al·$m^{-3}$ and a contact time of 15 min is maintained, obtaining a theoretical S/L separation efficiency of 95 %. The section B1 is aimed at increasing the algae concentration up to 5 g TSS·$L^{-1}$. Each CFS tank is fed by a feeding pump operated continuously. After each CFS tank, a harvesting pump is employed to convey the pre-concentrated biomass to the subsequent harvesting unit (section B2), while a recirculation pump sends the liquid fraction back to section A or to the main line of the WWTP. In section B2, the pre-concentrated biomass stream is equalized in a storage tank, from which it is sent, by means of a pump, to a centrifuge operated for 6 h·$d^{-1}$, to obtain an algal paste at a final concentration of 200 g TSS·$L^{-1}$, coherently with previous findings [21,29]. After centrifugation, the liquid fraction is fed to a storage tank, from which the effluent is sent back to the main water line of the WWTP.

**Calculation of CAPEX, OPEX and cost savings**

To provide a realistic assessment of biomass production costs, capital expenditures (CAPEX) and operational expenditures (OPEX) were calculated for each section, as detailed below. When reliable estimates of the costs were not available, Lang multipliers were applied to provide a preliminary estimate of the overall plant cost, as proposed in several techno-economic assessments of chemical engineering plants and microalgal biorefineries [32,33]. Lang factors were applied to the following items of expenditure: installation costs, service facilities, construction expenses, engineering and supervision, contractor's fee, contingencies, and maintenance.

CAPEX calculation

The relevant CAPEX for this analysis are described in this section. The land costs include the acquisition of the land, and its preparation for installing the RWPs and the accessory elements. The land cost is assumed according to the average price of agricultural land in Lombardy for the year 2020 [34]. Equipment costs include the purchase of the following items: the paddlewheels, feeding and recirculation pumps, instrumentation/control units for the RWPs (for sections A1 and A2); the CFS tanks, mixers, and pumps (for section B1), and the centrifuge (for section B2). The depreciation of investments is evaluated considering a lifetime for the plant equal to 20 years and is based on Lang factors, according to Ruiz et al. [33].

Equipment costs for which direct quotations were not available, were scaled based on the cost of quoted reference items, according to the

**Table 4**
Comparison of biomass productivity and nutrient removal efficiencies obtained in this study with the literature.

| REFERENCE | INFLUENT WASTEWATER | MAIN ALGAL GENERA | $P_A$ [g $TSS \cdot m^{-2} \cdot d^{-1}$] | $\eta_{TAN}$ [%] | $\eta_{PO4}$ [%] |
|---|---|---|---|---|---|
| [52] | Piggery WW | *Anabena, Dolichospermium* | 11.3 – 28.8 | 93 – 96 | 52 – 58 |
| [53] | Piggery WW | *Chlorella, Scenedesmus, Nizschia* | – | 96 – 99 | – |
| [21] | Piggery WW | *Chlorella, Scenedesmus* | 10.7 ± 6.5 | 90 ± 10 | 90 ± 27 |
| [54] | Municipal WW | *Scenedesmus* | 20 – 26 | – | – |
| [48] | Municipal WW | *Pedastrium* | 9–16.7 | 74 – 77 | – |
| [55] | Digestate (food processing WW) | *Chlorella, Scenedesmus, Dictyosphaerium* | 2 – 9 | 70–94 | 16 – 59 |
| [49] | Digestate (food processing WW) | *Chlorella* | 2.5 – 11.8 | – | 36 – 86 |
| [46] | Digestate (solid waste) | *Chlorella, Scenedesmus, Synecochoccus, Synecocystis* | 1.2 – 6.9 | 15 – 92 | 78 – 97 |
| [14] | Digestate (piggery WW) | *Chlorella, Scenedesmus* | 3 – 16 | 80 ± 13 | – |
| [56] | Digestate (piggery WW) | *Chlorella, Scenedesmus* | – | 79 ± 15 | – |
| [57] | Digestate (piggery WW) | *Scenedesmus, Chroococcus* | 6.2 ± 1.0 | 99.7 ± 0.7 | – |
| [16] | Digestate (piggery WW) | *Chlorella, Scenedesmus* | 3.6 – 22 | 3 – 86 | 9 – 57 |
| [58] | Digestate (piggery WW) | *Chlorella, Scenedesmus* | 4.2 | 69 | – |
| [59] | Digestate (municipal WW) | *Nannochloropsis* | 5 – 14 | 20 – 60 | 20 – 85 |
| [51] | Digestate (municipal WW) | *Chlorella* | 15 | 99 – 100 | 85 – 92 |
| [60] | Digestate (municipal WW) | *Ankistrodesmus, Micractinium* | 3.8 – 8 | – | 32 – 50 |
| [50] | Digestate (municipal WW) | *Scenedesmus* | 24 | 55 | – |
| [15] | Digestate (municipal WW) | *Chlorella, Scenedesmus, Chlamydomonas* | 3.4 – 8.4 | 86 ± 7 | 71 ± 10 |
| [61] | Digestate (municipal WW) | *Pseudoanabena, Nannochloropsis, Halamphora, Geitlerinema* | 32.4 | 80 – 90 | 80 – 90 |
| [62] | Digestate (municipal WW) | *Scenedesmus* | 5 – 22.9 | 94 | 90.6 |
| This study (year 2020) | Digestate (municipal WW) | *Chlorella, Scenedesmus* | 11.8 ± 7.6 | 84.5 ± 7.8 | 36.9 ± 12.1 |
| This study (year 2021) | Digestate (municipal WW) | *Chlorella, Scenedesmus* | 8.4 ± 5.7 | 85.4 ± 8.1 | 35.8 ± 18.7 |
| This study (overall) | Digestate (municipal WW) | *Chlorella, Scenedesmus* | 9.5 ± 6.4 | 85.1 ± 7.9 | 36.2 ± 16.7 |

exponential rule that is typically adopted in chemical engineering projects (**Equation (7)**):

$$\frac{Cost_A}{Cost_B} = \left(\frac{Size_A}{Size_B}\right)^n \tag{7}$$

where: $Cost_A$ [€] and $Size_A$ are the cost and the size of a generic item to be quoted, $Cost_B$ [€] and $Size_B$ are the cost and size of a similar item for which a reliable quote is available, and n [-] is the cost exponent, typically varying in the range 0.45–0.85 [38,39].

OPEX calculation

Energy costs include the expenses for running all the electromechanic devices, i.e., the feeding pumps and the paddlewheels in sections A1 and A2, the mixers, harvesting and recirculation pumps, and the centrifuge in sections B1 and B2. The reagents costs include the NaOH required to correct the alkalinity in section B2 and the flocculant for section B1. Additional nutrients costs were not considered, since nitrogen and phosphorus are provided by the digestate, and $CO_2$ is freely available from the biogas upgrading section of the plant. Finally, labour costs are calculated accounting to similar case studies [21,40], and the microalgae production plant is operated by two field operators, a supervisor and a plant manager.

Cost savings and carbon credits

In the economic analysis, the saved cost due to the removal of TAN and $PO_4^{3-}$ was computed. To evaluate the cost saved due to ammoniacal nitrogen removal in the algae-bacteria unit, the TAN load that should not be oxidized in the main line of the WWTP was computed as the sum of the nitrogen in the algal biomass (assuming a nitrogen content in the algal biomass equal to 6.6 %, on a mass basis) and the nitrified TAN. Assuming an energy consumption for nitrogen removal in the WWTP of 6.5 $kWh \cdot kg\ N^{-1}$ [41], the energy saving for nitrification could be calculated. The savings related to the removal of orthophosphate was calculated assuming a P removal cost of 2.4 €$\cdot kg\ P^{-1}$ [42]. Finally, the credits obtained through the biofixation of $CO_2$ by the algae-bacteria consortium were quantified by assuming a stoichiometric content of 1.88 kg $CO_2 \cdot kg\ DW^{-1}$ and a carbon credit of 83 €$\cdot t\ CO_2^{-1}$, i.e., equal to the 2022 average calculated from the EU Emissions Trading System data [43].

Cost actualization

To account for inflation, the actual value of a currency considering was calculated by using the European Union Consumer Price Index (EU-HICP) provided by Eurostat [44].

### 2.3.3. Sensitivity and scenario analysis

A sensitivity analysis was conducted, by considering the variation of the most important parameters having a relevant impact on the final biomass production cost. These parameters are the biomass productivity (that can vary according to different plant operations and local climate conditions) as well as the overall OPEX and CAPEX. A variation of ± 20 % was considered for these parameters, to identify their effect on the final biomass production and wastewater treatment costs.

## 3. Results and discussion

### 3.1. Pilot-scale microalgae cultivation and digestate treatment

#### 3.1.1. Microalgal productivity and communities

Fig. 4 shows the trends of the biomass parameters during the two monitoring campaigns. Results are expressed in terms of TSS and microscope cell counts. In 2020 campaign (Fig. 4A), after an initial growth period lasting approximately 20 days, biomass concentration was quite stable, reaching a TSS concentrations of approximately 0.55–0.80 g $TSS \cdot L^{-1}$ (with microalgal cell counts of 4.6 – 5.6 $\cdot 10^6$ $cells \cdot mL^{-1}$). During the last 20 days of operation, the biomass concentrations decreased, in response to the sub-optimal temperature and irradiance conditions. Indeed, during this period, the maximum daily irradiance reached in the outdoor system decreased well below 700 $\mu mol \cdot m^{-2} \cdot s^{-1}$, frequently not even reaching 200 $\mu mol \cdot m^{-2} \cdot s^{-1}$. Concurrently, the average daily temperature was always lower than 20 °C, reaching minimum values of 2 °C in October. During the 2021 monitoring campaign (Fig. 4B), from May to August, more stable conditions were achieved for biomass concentration, with average TSS concentrations of 0.59–0.90 g $TSS \cdot L^{-1}$ (corresponding to optical densities of 0.5 – 0.8 and microalgae counts of 1.7 – 4.2 $\cdot 10^6$ $cells \cdot mL^{-1}$). A sudden culture crash with algae flocculation was experienced at the end of September. This was probably due to the presence of residual flocculant in the influent digestate batch, though this hypothesis could not be experimentally verified. The rapid and unaccounted tendency of microalgae to flocculate was also combined to the appearance of microalgae predators (mainly, protozoa), that facilitated a further drop in the biomass concentration, up to exceptionally low values (below 0.1 g $TSS \cdot L^{-1}$, corresponding to a loss of approximately 83 % of the algal cells in the suspension). After this event, the system was inoculated again with an algal consortium that was previously grown in the laboratory (composed of *Chlorella* and *Scenedesmus* spp.) on a new batch of digestate. Following the re-inoculation, the

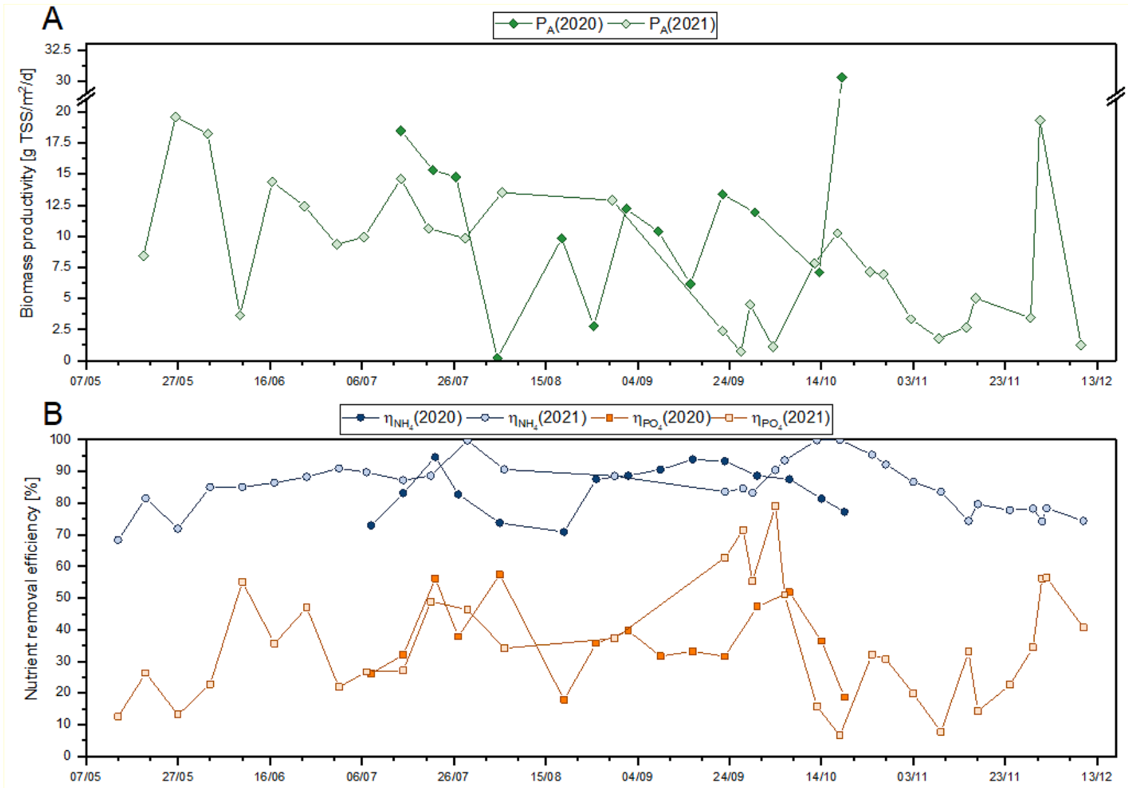


**Fig. 5.** Evolution of the algal biomass productivity (A) and nutrient removal efficiencies (B) during the two monitoring campaigns.

biomass concentration reached levels comparable, or even higher, than those obtained in during the same period of 2020. After reaching the highest number of cells in the suspension at the end of October (6.63 · $10^6$ cells·mL$^{-1}$), the biomass concentrations steadily decreased until December due to the sub-optimal weather conditions (average daily irradiance below 100 μmol·m$^{-2}$·s$^{-1}$ and air temperature in the range 0 – 6 °C). The lateral panels of the greenhouse were then installed, and the biomass concentration experienced a slight increase until the end of the experimentation (up to 0.23 – 0.37 g TSS·L$^{-1}$), due to the increased temperature in the pond.

Regarding the composition of the microalgae community, Fig. 4 shows that the dominant algae species were *Chlorella* and *Scenedesmus* spp., consistently with the results reported in the literature (Table 4). These two ubiquitous species are typically found in wastewater and digestate treatment systems [45,46]. During the first phase of 2020, *Scenedesmus* sp. was dominant while *Chlorella* sp. took over from September onward, together with other unidentified green algae species (up to 43 % of the total number of cells, Fig. 4B). In 2021, the occurrence of algae other than *Chlorella* and *Scenedesmus* spp. was negligible. A shift from the prevalence of *Scenedesmus* sp., to the complete dominance of *Chlorella* sp. was observed during the first two weeks; *Chlorella* prevailed until the end of September (Fig. 4D). After the system was restarted with the new inoculum (containing both species), *Scenedesmus* sp. became the dominant algal population, with peaks up to 90 % of the total number of cells. Concurrently, other species showed up, during the second part of the 2021 campaign, though remaining in very low concentrations (less than 5 % of the total algal biomass). Although the reasons for the prevalence of one genus over another remain to be defined, it can be assumed that environmental conditions (mostly, irradiance and temperature) are playing a key role.

Fig. 5 A-B reports the trend of the total biomass productivity ($P_A$) during the two monitoring campaigns. As shown in Table 4, in both monitoring campaigns, the system achieved productivities that typically fall in the range of literature values. In 2020, an average productivity of 11.8 ± 7.6 g TSS·m$^{-2}$·d$^{-1}$ was reached, corresponding to approximately 61.1 ± 39.5 g TSS·m$^{-3}$·d$^{-1}$. During this year, the photosynthetic efficiency was 1.53 ± 1.73 %, that is comparable to the values reviewed by Norsker et al. [47]. In 2021, on average, a lower productivity was reached, since the campaign was extended until winter and because of the biomass concentration drop that occurred in September 2021. The average productivity considering the entire experimental period was 8.4 ± 5.7 g TSS·m$^{-2}$·d$^{-1}$ (41.6 ± 28.1 g TSS·m$^{-3}$·d$^{-1}$). However, a productivity higher than that obtained in 2020 was obtained when considering only the data before the culture crash (12.1 ± 4.2 g TSS·m$^{-2}$·d$^{-1}$ until September). Considering the period following the culture crash (from September to December), the average productivity was 5.2 ± 4.8 g TSS·m$^{-2}$·d$^{-1}$. On average, for the year 2021, the photosynthetic efficiency was 1.97 ± 2.85 %. The values obtained in the present monitoring campaigns are comparable with the results obtained in the treatment of agro-zootechnical and urban wastewater [14,48,49], also being higher than the values previously obtained in the same treatment system [15]. In some cases, a higher productivity could be achieved using digestates derived from urban wastewater [50,51] or from piggery wastewaters [21,52]. However, discrepancies with other studies in the literature are likely to be attributed to the different climate conditions as well as to the case specific wastewater characteristics.

### 3.1.2. *Nutrient removal performance and efficiency*

The concentrations of nitrogen compounds were monitored over time to calculate the removal rates and efficiencies of TAN and orthophosphates. During the two consecutive years, the nitrogen loading rate (NLR) was 19.3 ± 2.5 and 31.7 ± 7.4 g N·m$^{-3}$·d$^{-1}$ in 2020 and 2021, respectively, resulting in a similar trend for nitrogen removal also due to the similar weather conditions recorded during the two years. A relatively low concentration of TAN (typically lower than 50 mg N·L$^{-1}$) was always released with the effluent, while in a few cases, corresponding to the start-up phases or during sub-optimal weather conditions, the effluent TAN was slightly higher (up to a maximum of 70 mg N·L$^{-1}$).

**Table 5**
Main design hypothesis and results for CAPEX calculation.

| SECTION | PARAMETER | UNIT | VALUE | REFERENCE / NOTES |
|---|---|---|---|---|
| GENERAL DATA | Specific cost of liner | €·m$^{-2}$ | 4.7 | [69] |
| | Specific cost of concrete | €·m$^{-3}$ | 100 | [21] |
| | Specific cost of pipes/wires | €·m$^{-1}$ | 31 | [70] |
| | Cost of civil works | € | 42,089 | Based on 70,000 € for 5.5 ha |
| | Piping length | m | 594 | Based on 3 m distance among RWPs |
| | Wiring length | m | 297 | Assumed as half of the piping length |
| | Cost of piping and wiring | € | 27,244 | Based on 3 m distance among RWPs |
| | Land cost | €·ha$^{-1}$ | 47,996 | Average agricultural land cost in Lombardy [34] |
| | Cost exponent for civil work, piping/wiring, pump, centrifuge, instrumentation | – | 0.65 | [39] |
| | Cost exponent for paddlewheels, mixers, tanks | – | 0.45 | [39] |
| | Number of pumps | . | 13 | Based on process layout |
| | Feeding, recirculation and harvesting pumps cost | € | 23,572 | Based on 1115 €·unit$^{-1}$ for 3.6 m$^3$·h$^{-1}$ pump |
| | Number of storage tanks | – | 2 | Based on process layout |
| | Cost for storage tanks | € | 461 | Based on 811 € for 754 m$^3$ |
| A1 – INOCULATION PONDS | Cost of paddlewheels | € | 15,063 | Based on 40,000 € for 2 acres installation |
| | Cost of liner | € | 2,172 | Calculated |
| | Height of concrete walls | m | 0.3 | Considering an allowance of 10 cm |
| | Width of concrete walls | m | 0.03 | Assumed |
| | Total concrete volume | m$^3$ | 2.7 | Calculated |
| A2 – CULTIVATION PONDS | Cost of paddlewheels | € | 210,351 | Based on 40,000 € for 2 acres installation |
| | Cost of liner | € | 97,745 | Calculated |
| | Height of concrete walls | m | 0.3 | Considering an allowance of 15 cm |
| | Width of concrete walls | m | 0.05 | Assumed |
| | Total concrete volume | m$^3$ | 94.1 | Calculated |
| | Instrumentation cost | € | 27,912 | Based on 1000 €·unit$^{-1}$ for 100 m$^3$ RWP |
| B1 – COAGULATION, FLOCCULATION, SEDIMENTATION | CFS tank cost | € | 100,889 | Based on 125,000 €·unit$^{-1}$ for 100 m$^3$ tank |
| | Mixer cost | € | 8,071 | Based on 10,000 €·unit$^{-1}$ for 100 m$^3$ tank |
| B2 – CENTRIFUGATION | Centrifuge cost | € | 54,521 | Based on 250,000 €·unit$^{-1}$ for 80.0 m$^3$·h$^{-1}$ centrifuge |

These resulting performances suggest that the system could be efficiently adopted as a side-stream process for nitrogen removal from digestate, though effluent concentrations would not allow for the direct discharge of the treated digestate to the receiving water body. In both campaigns, a substantial proportion of the influent nitrogen was nitrified (80.6 ± 37.0 % in 2020 and 60.0 ± 31.8 % in 2021), with high nitrification rates reaching an average value on the entire experimentation of 29.9 ± 10.2 g N-$NH_4^+$·m$^{-3}$·d$^{-1}$. Partial nitrification was observed, especially in 2020, as confirmed by the low concentrations of nitrate obtained (typically below 60 mg N·L$^{-1}$). Only at the end of the 2021 trial, nitrification was almost complete, with an outlet concentration of nitrate over 200 mg N·L$^{-1}$ (i.e., up to 95% of the influent TAN), probably thanks to the combination of the higher ALK to TAN ratio in this year, and the milder competition between nitrifiers and microalgae, caused by the lower algal growth rate recorded in the same period. Nitrite accumulation in algae-bacteria systems treating anaerobic digestion effluents and other wastewaters has been previously observed in the literature [15,56], though a solid explanation of this phenomenon is still lacking. Partial nitrification is often attributed to the presence of FAN, that is formed in abundance at high pH, temperature, and TAN concentrations, which are common conditions in algae-bacteria systems. Free ammonia is indeed a strong inhibitor for the growth of autotrophic microorganisms, including microalgae and cyanobacteria [24,63], as well as AOB and NOB [64,65]. However, the maximum FAN concentration was always below 0.3 mg N·L$^{-1}$, which is smaller than reported inhibitory levels for NOB [66]. Other factors, such as the competition for common nutrients may have played a role in shaping the nitrifying community. Inorganic carbon limitation is a possible explanation for the low NOB activity, as the digestate is characterized by an alkalinity shortage, making it difficult to store inorganic carbon in the bulk [16]. On the other hand, the tolerance to environmental conditions could have played a role in favoring AOB, as the temperature and DO concentration in the pond were closer to optimal values for AOB than for NOB [67].

On the overall, the system achieved high TAN removal efficiencies (Fig. 5C-D). During the experiments conducted in 2020, the TAN removal efficiency averaged 84.5 ± 7.8 %, always being in the range 71–95 %, and a similar result was achieved in 2021, when the mean removal efficiency was 85.4 ± 8.1 % (range: 68 – 100 %). The values obtained are consistent with previous work reported in the literature (Table 4). TAN removal was comparable, or even higher, than those reported in many previous studies describing the phyco-remediation of urban wastewater [48], digestates from municipal wastewaters [50,59], and digestates from agro-industrial wastewaters [14,56]. Only in a few cases, TAN removal reached higher values, mostly due to the combination of high HRTs and NLRs [52,53,57,62]. The calculation of oxygen production by microalgae and oxygen consumption by nitrifying bacteria also confirmed that the oxygen demand for TAN oxidation was mainly provided by photo-oxygenation and/or oxygen transfer, in complete absence of external aeration, allowing for a large energy saving and the reduction of operating costs for digestate nitrification (data not shown).

The trends in orthophosphate removal during the two monitoring campaigns are shown in Fig. 5C-D. The outlet $PO_4^{3-}$ concentrations were low (4–7 mg P·L$^{-1}$), however it must be considered that the PLR was also quite low (0.72 ± 0.13 g P·m$^{-3}$·d$^{-1}$ in 2020, and 1.32 ± 0.34 g P·m$^{-3}$·d$^{-1}$ in 2021), due to the low concentrations in the digestate. As shown in Fig. 5, the resulting removal efficiency was on average 36.9 % ± 12.1 % during 2020 (varying between 17.9 and 57.5 %), and 35.8 ± 18.7 % during 2021 (with a wider range of variation of 6.5 – 79.1 %). In terms of $PO_4^{3-}$ removal rates, the system was able to remove an average of only 0.31 ± 0.29 g P-$PO_4^{3-}$·m$^{-3}$·d$^{-1}$ in 2020, and 0.52 ± 0.44 g P-$PO_4^{3-}$·m$^{-3}$·d$^{-1}$ in 2021. Therefore, it can be concluded that the algae/bacteria consortium was less efficient in P removal, as it is commonly reported in the literature (see Table 4), regardless of the reactor type, wastewater origin, and weather characteristics [55,59,60]. On the other hand, orthophosphate removal efficiencies obtained in some recent

**Table 6**
Main design hypothesis and results for OPEX calculation.

| SECTION | PARAMETER | UNIT | VALUE | REFERENCE / NOTES |
|---|---|---|---|---|
| GENERAL DATA | Cost of electricity | €·kWh$^{-1}$ | 0.1171 | Based on the average price for non-household consumers in Italy [34] |
| | Efficiency of paddlewheel motor | % | 85 | [29] |
| | Increased power consumption for $CO_2$ sparging | % | 15 | [29] |
| | Specific paddlewheel consumption | W·m$^{-2}$ | 0.35 | [29] |
| | Number of field operators | – | 2 | Assuming 5 RWP·operator$^{-1}$ |
| | Number of supervisors | – | 1 | Assumed |
| | Number of plant managers | – | 1 | Assumed |
| | Salary of field operators | €·h$^{-1}$ | 13.1 | Assuming a factor of 3 on a base salary of 4.4 €·h$^{-1}$ |
| | Salary of supervisors | €·h$^{-1}$ | 18.8 | Assuming a factor of 4.3 on a base salary of 4.4 €·h$^{-1}$ |
| | Salary of plant managers | €·h$^{-1}$ | 29.3 | Assuming a factor of 6.7 on a base salary of 4.4 €·h$^{-1}$ |
| | Work shift | h·d$^{-1}$ | 6 | Assumed |
| | Installed power for feeding, recirculation and harvesting pumps | kW | 5.7 | Calculated |
| | Energy consumption for feeding, recirculation and harvesting pumps | kWh·y$^{-1}$ | 37,615 | Calculated |
| A1 – INOCULATION PONDS | Installed power for paddlewheels | kW | 0.2 | Calculated |
| | Energy consumption for paddlewheels | kWh·y$^{-1}$ | 1,233 | Calculated |
| A2 – CULTIVATION PONDS | Installed power for paddlewheels | kW | 9.2 | Calculated |
| | Energy consumption for paddlewheels | kWh·y$^{-1}$ | 60,423 | Calculated |
| | NaOH required | kg·d$^{-1}$ | 365 | Calculated to reach 25 mM alkalinity in the digestate |
| | NaOH cost | €·kg$^{-1}$ | 0.4 | [16] |
| B1 – COAGULATION, FLOCCULATION, SEDIMENTATION | Flocculant required | kg·d$^{-1}$ | 5.5 | Calculated |
| | Flocculant cost | €·kg$^{-1}$ | 0.23 | [71] |
| | Specific energy consumption for mixers | kWh·(m$^3$·d$^{-1}$)$^{-1}$ | 0.0014 | [29] |
| | Energy consumption for mixers | kWh·y$^{-1}$ | 1,681 | Calculated |
| B2 – CENTRIFUGATION | Specific energy consumption for centrifuge | kWh·m$^{-3}$ | 1.3 | [40] |
| | Energy consumption for centrifuge | kWh·y$^{-1}$ | 65,689 | Calculated |

experiences were higher than those reported here [15,46,49], possibly due to the fact that, in these studies, PLRs were higher and the environmental conditions were more suitable for microalgae growth than in the current case study.

On the overall, it can be concluded that the results obtained in this study confirmed the suitability of the treatment system to efficiently remove ammoniacal nitrogen and valorise the chemical energy content of the digestate, while producing a biomass that is dominated by algal species typically rich in carbohydrates, lipids, and proteins [68], therefore being suitable for further valorisation. The variability of the effluent concentrations of nutrients, and especially the low removal efficiencies obtained for phosphates suggest that the system is mostly suitable for side-stream treatment at these latitudes, since low nutrient concentrations in the effluent cannot be guaranteed, and regulatory limits may be exceeded.

### 3.2. Techno-economic assessment and scenario analysis

Based on the pilot data provided in **Section 2.3**, a comprehensive techno-economic assessment was conducted, to evaluate the feasibility of scaling-up the process of microalgae cultivation on digestate by assessing costs of biomass production and of wastewater treatment. To calculate the savings of the WWTP, costs deriving from the oxidation of the TAN contained in the digestate and for phosphate removal were accounted on the baseline scenario. In the framework of the desirable implementation of a carbon–neutral economy, $CO_2$ compensation credits were also included. On the contrary, no revenues from biomass selling were considered, limiting the economic considerations to the biomass production only and allowing to identify the best option for biomass valorisation, according to the expected market price for different bio-products. The detailed CAPEX and OPEX costs resulting from the TEA of the baseline case are reported in Table 5 and Table 6, respectively.

#### 3.2.1. Baseline case study

By considering the expected average productivity based on the photosynthetic efficiency over the 274 d·y$^{-1}$ of plant operation (9.9 g TSS·m$^{-2}$·d$^{-1}$), a biomass production cost of 4.3 €·kg TSS$^{-1}$ is obtained (Table 7). This cost is comparable to the previous studies describing techno-economic assessments on microalgal cultivation in RWPs using wastewaters. For example, Al Ketife et al. [72] reported biomass production costs of 0.5 €·kg DW$^{-1}$, when treating municipal wastewaters using *Nannochloropsis* sp., while a recent study comparing the economics of microalgal cultivation in different types of wastewaters in large-scale RWPs reported costs ranging from 0.4 to 0.8 €·kg DW$^{-1}$ [73]. Recently, a similar biomass production cost of 1.9 €·kg TSS$^{-1}$, was reported for the treatment of piggery wastewaters in large scale farms, while at a lower scale, this cost increased up to 10.3 €·kg TSS$^{-1}$ [21]. It should be stressed that biomass production costs largely depend on the type of cultivation reactor considered, wastewater characteristics, climate, and available area, therefore a direct comparison is not straightforward [9,73]. For example, the production cost for open ponds are in the range 4.7 – 12.7 €·kg DW$^{-1}$ [74], while they raise to 98 – 610 €·kg DW$^{-1}$ for closed PBRs [75].

As shown in Fig. 6, the yearly cost is mostly due to OPEX (accounting for 285.2 k€·y$^{-1}$, or 79.3 % of the yearly costs), with a minor contribution of CAPEX (74.4 k€·y$^{-1}$, representing 20.7 % of yearly expenses). A more detailed analysis of the cost breakdown allows to highlight that the major contribution in terms of OPEX is given by labour, and overheads (42.8 % and 27.6 %, respectively), followed by materials, and maintenance (13.2 % and 7.3 %, respectively). In terms of CAPEX share, yearly costs mostly come from the investment depreciation (85.3 %), followed by the interests and land cost (6.8 % and 6.4 %, respectively). Regarding the overall benefits from nutrient and $CO_2$ removal (85.1 k€·y$^{-1}$), nitrogen removal contributes to 81.2 % of the overall saving, followed by $CO_2$ fixation credits (11.6 %) and P removal (7.2 %).

In terms of digestate treatment, the cost for the proposed (Fig. 7)

**Table 7**
Summary of costs for the different scenarios identified from the sensitivity analysis (best-case: 20% increase in the productivity and 20% decrease in the OPEX and CAPEX; worst-case: 20% decrease in the productivity and 20% increase in the OPEX and CAPEX).

| ITEM | PARAMETER | UNIT | BEST-CASE | BASELINE | WORST-CASE | REFERENCE / NOTES |
|---|---|---|---|---|---|---|
| DIRECT COSTS (DC) | Major equipment costs (MEC) | € | 433,366 | 522,527 | 601,835 | Costs for paddlewheels, concrete, liner, pumps, tanks, mixers, and centrifuge |
| | Installation costs | € | 86,673 | 104,505 | 120,367 | Calculated as 20 % of MEC |
| | Instrumentation and control | € | 22,330 | 27,912 | 33,494 | Equal to the costs for instrumentation and control |
| | Piping | € | 18,163 | 18,163 | 18,163 | Equal to the costs for piping |
| | Electrical | € | 9,081 | 9,081 | 9,081 | Equal to the costs for wiring |
| | Land improvement | € | 33,671 | 42,089 | 50,507 | Equal to the cost of civil works |
| | Service facilities | € | 86,673 | 104,505 | 120,367 | Calculated as 20 % of MEC |
| | Total DC | € | 689,958 | 828,782 | 953,813 | Calculated as the sum of DC |
| INDIRECT COSTS (IC) | Construction expenses | € | 68,996 | 82,878 | 95,381 | Calculated as 10 % of DC |
| | Engineering and supervision | € | 130,010 | 156,758 | 180,550 | Calculated as 30 % of MEC |
| | Total IC | € | 199,006 | 239,636 | 275,932 | Calculated as the sum of IC |
| OTHER COSTS (OC) | Contractor's fee | € | 34,498 | 41,439 | 47,691 | Calculated as 5 % of DC |
| | MEC contingency | € | 133,344 | 160,263 | 184,462 | Calculated as 15 % of the sum of DC and IC |
| | Total OC | € | 167,842 | 201,702 | 232,152 | Calculated as the sum of OC |
| CAPEX | Depreciation | $€\cdot y^{-1}$ | 52,840 | 63,506 | 73,095 | Calculated as the sum of DC, IC and OC, divided by the lifetime of the plant |
| | Interest | $€\cdot y^{-1}$ | 4,227 | 5,080 | 5,848 | Calculated as 8 % of the depreciation |
| | Property tax | $€\cdot y^{-1}$ | 571 | 686 | 789 | Calculated as 1 % of the sum of depreciation and interest |
| | Insurance | $€\cdot y^{-1}$ | 342 | 412 | 474 | Calculated as 0.6 % of the sum of depreciation and interest |
| | Land | $€\cdot y^{-1}$ | 3,801 | 4,752 | 5,702 | Calculated as the cost of land divided by the lifetime of the plant |
| | Total CAPEX | $€\cdot y^{-1}$ | 61,782 | 74,435 | 85,907 | Calculated as the sum of CAPEX |
| OPEX | Energy | $€\cdot y^{-1}$ | 16,083 | 20,104 | 24,125 | Calculated from major equipment consumption |
| | Labour | $€\cdot y^{-1}$ | 97,706 | 122,133 | 146,559 | Calculated as the sum of labour cost |
| | Raw materials | $€\cdot y^{-1}$ | 30,049 | 37,561 | 45,073 | Calculated from mass balances |
| | Maintenance | $€\cdot y^{-1}$ | 13,868 | 20,901 | 28,888 | Calculated as 4 % of MEC |
| | Operating supplies | $€\cdot y^{-1}$ | 148 | 231 | 332 | Calculated as 0.4 % of the sum of electricity and raw materials |
| | Contingencies | $€\cdot y^{-1}$ | 3,606 | 5,634 | 8,113 | Calculated as 15 % of the sum of raw materials |
| | Overheads | $€\cdot y^{-1}$ | 49,093 | 78,669 | 115,795 | Calculated as 55 % of the sum of labour and maintenance |
| | Total OPEX | $€\cdot y^{-1}$ | 210,552 | 285,232 | 368,886 | Calculated as the sum of OPEX |
| SAVINGS | Energy for nitrification | $€\cdot y^{-1}$ | 69,807 | 69,174 | 68,540 | Calculated based on energy saved for nitrification |
| | P removal cost | $€\cdot y^{-1}$ | 6,096 | 6,096 | 6,096 | Calculated based on phosphate removal efficiency |
| | $CO_2$ credits | $€\cdot y^{-1}$ | 11,849 | 9,875 | 7,900 | Calculated based on the carbon credit |
| | Total savings | $€\cdot y^{-1}$ | 87,753 | 85,144 | 82,535 | Calculated as the sum of savings |
| SPECIFIC COSTS | Biomass production costs | $€\cdot kg\ TSS^{-1}$ | 2.4 | 4.3 | 7.4 | Calculated based on the biomass productivity |
| | Digestate treatment cost | $€\cdot m^{-3}$ | 1.5 | 2.7 | 4.7 | Calculated based on the treated digestate |
| | Nitrogen removal cost | $€\cdot kg\ N^{-1}$ | 7.0 | 12.5 | 21.1 | Calculated based on the removed nitrogen |

process is 2.7 $€\cdot m^{-3}$, that is well comparable to the results of Chaudry [73] who obtained treatment costs of 0.2 – 1.9 $€\cdot m^{-3}$, and of Ansari et al. [76], reporting a cost of 0.9 $€\cdot m^{-3}$ for municipal wastewater treatment. Even if conventional wastewater treatment costs typically range from 0.1 to 0.5 $€\cdot m^{-3}$ [77–79], these costs are strongly influenced by the specific influent composition and process configuration, so they are hardly comparable. When referring to a more robust indicator, such as the specific nitrogen removal cost, the proposed process seems to be a very promising technology with a cost of 12.5 $€\cdot kg\ N^{-1}$, which is similar to previously reported costs for piggery wastewater phyco-remediation, i.e., 4.3–23 $€\cdot kg\ N^{-1}$ [21], and in the same range of conventional bioprocesses, typically ranging from 1.5 to 14.7 $€\cdot kg\ N^{-1}$, depending on the applied technology and influent characteristics [80,81].

### 3.2.2. Sensitivity and scenario analysis

The sensitivity analysis allowed to identify the parameters having the highest influence on the final biomass production cost. The variation of the productivity had a large impact on the final cost. Indeed, a 20 % increase in the productivity would result in a reduction of the production cost to 3.8 $€\cdot kg\ TSS^{-1}$ (-13.3 % compared to the baseline scenario), while a 20 % decrease in the productivity would result in an increase of the cost up to 5.2 $€\cdot kg\ TSS^{-1}$ (+19.7 %). On the other hand, increasing the total OPEX and CAPEX also had a strong effect of the biomass production cost, with the variation in total OPEX having more influence than the CAPEX. Indeed, a 20 % increase in the OPEX would result in a production cost of 5.6 $€\cdot kg\ TSS^{-1}$ (corresponding to a 28.2 % increase), while the same increment in the CAPEX would result in a cost of 4.7 $€\cdot kg\ TSS^{-1}$ (i.e., a percentage increase of 7.6 %). When looking at the sensitivity results obtained decreasing the operational and capital expenditures of 20 %, the overall costs would reduce to 3.2 $€\cdot kg\ TSS^{-1}$ and 4.0 $€\cdot kg\ TSS^{-1}$, respectively (representing a reduction of 25.7 % for the OPEX reduction, and 7.6 % when reducing the CAPEX).

Following the sensitivity analysis, two scenarios were considered in addition to the baseline case: i) a best-case scenario where a 20 % reduction in both OPEX and CAPEX are achieved, coupled to a 20 % increase in the productivity of the system, and ii) a worst-case scenario with a 20 % reduction in the productivity, coupled to the same increase for OPEX and CAPEX (Table 7). For the worst-case scenario, the biomass production cost can increase up to 7.4 $€\cdot kg\ TSS^{-1}$, while the digestate treatment cost and the specific nitrogen removal cost would reach 4.7 $€\cdot m^{-3}$ and 21.1 $€\cdot kg\ N^{-1}$, respectively. On the contrary, in the best-case scenario, the biomass production cost decreases to 2.4 $€\cdot kg\ TSS^{-1}$, and the resulting digestate treatment and nitrogen removal cost drop to 1.5 $€\cdot kg\ m^{-3}$ and 7.0 $€\cdot kg\ N^{-1}$, respectively. The results compare well to the most convenient biomass production costs reported to date in the literature [72,73,76,82,83]. This suggests that any effort in increasing the biomass productivity (e.g., by adopting mathematical growth models allowing to improve nutrient utilization or to better controlling the growth environment) would be compensated by a strong reduction in the production cost. In the same way, the related reduction of CAPEX and OPEX would have a very strong potential in spreading the promising phyco-remediation biotechnology, with the advantage of reducing

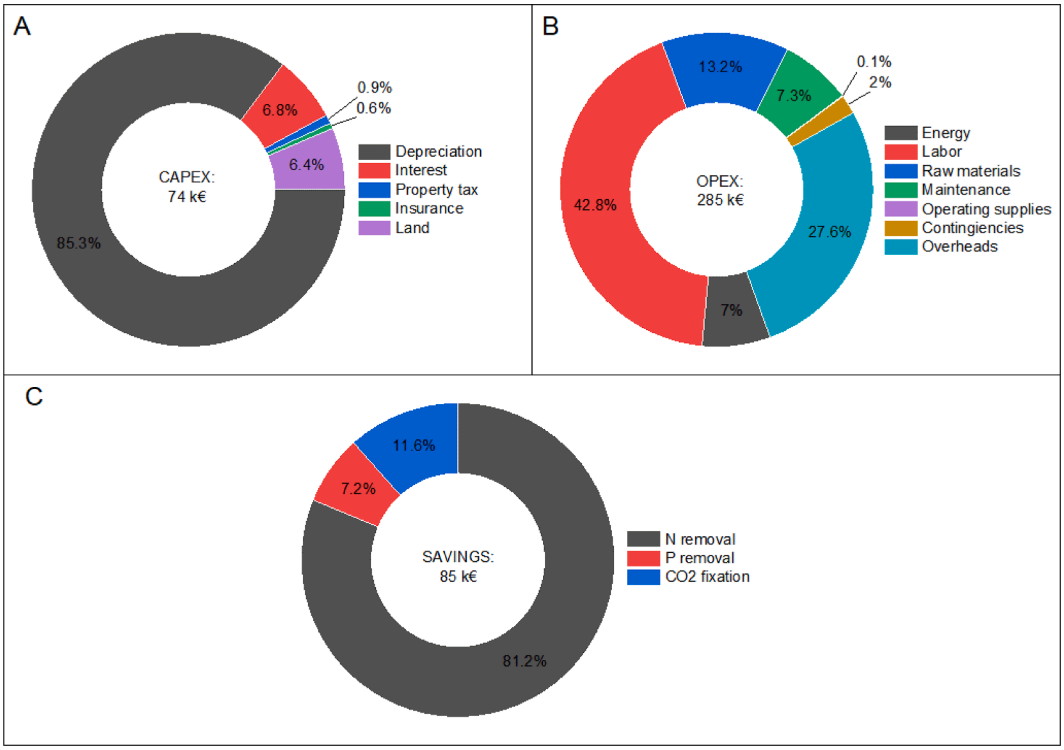


**Fig. 6.** Techno-economic assessment costs breakdown: A) CAPEX, B) OPEX, C) savings.

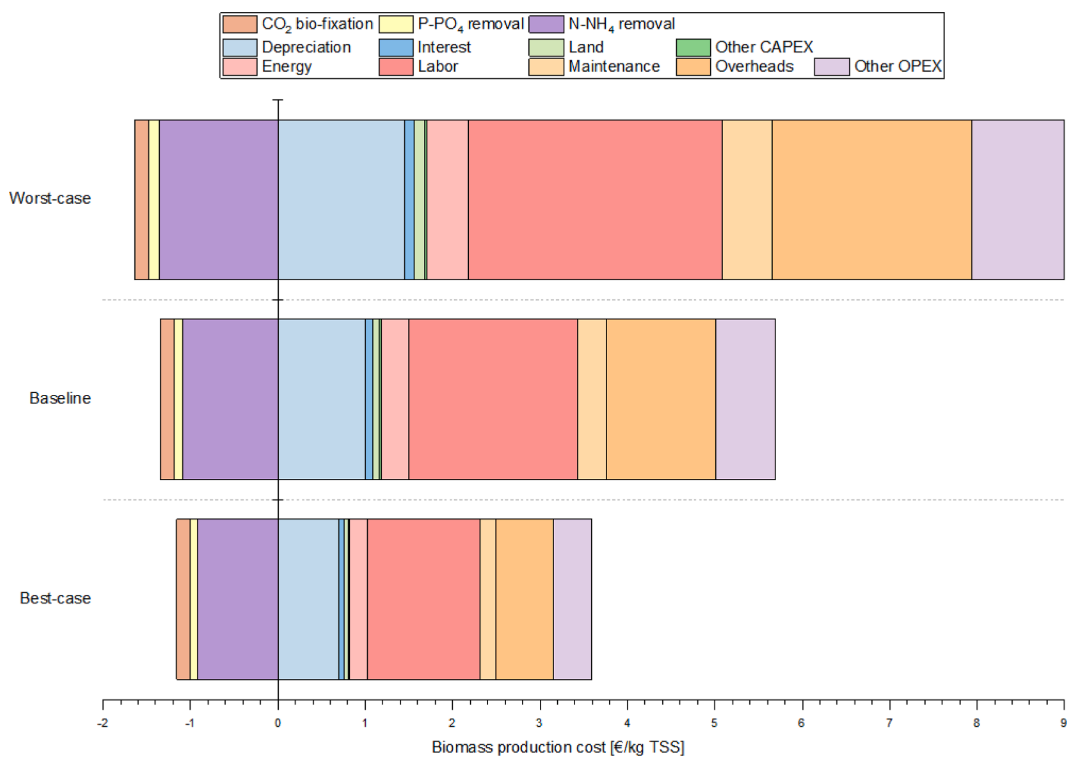


**Fig. 7.** Cost breakdown for the different scenarios identified from the sensitivity analysis (best-case: 20% increase in the productivity and 20% decrease in the OPEX and CAPEX; worst-case: 20% decrease in the productivity and 20% increase in the OPEX and CAPEX)."Other CAPEX" include: property tax and insurance; "Other OPEX" include: raw materials, operating supplies, and contingencies.

wastewater treatment costs and its environmental impacts, as well as promoting a circular and more sustainable utilization of the nutrients present in waste streams.

## 4. Conclusions

In this work, a pilot-scale microalgae-bacteria system treating the liquid phase of digestate, located in Northern Italy, was operated side-stream within a municipal wastewater treatment plant, to collect performance data. The average biomass productivity was 9.5 ± 6.4 g $TSS{\cdot}m^{-2}{\cdot}d^{-1}$, while TAN removal efficiency was 85.1 ± 7.9 %. Referring to the overall wastewater treatment process, the microalgae-bacteria unit allowed to save a considerable amount of energy for nitrification, while producing valuable biomass to be valorised in a circular economy perspective. Based on the pilot-scale results, a comprehensive techno-economic assessment and sensitivity analysis was conducted to evaluate the costs and feasibility of scaling-up the process to 2 ha, which is the area required to treat the nutrients contained in the available digestate flowrate. The resulting biomass production cost is 4.3 $€{\cdot}kg\ TSS^{-1}$, thus allowing for its exploitation as biostimulants or other bioproducts generation. The related digestate treatment cost is 2.7 $€{\cdot}m^{-3}$, corresponding to a specific nitrogen removal cost of 12.5 $€{\cdot}kg\ N^{-1}$. These costs would eventually reduce of approximately 44 % under a best-case scenario, in which the productivity is increased, and both the OPEX and CAPEX are reduced by 20 %. The results suggest that scaling up the process makes its cost comparable to conventional bioprocesses. The results reported in this study provide an important contribution to evaluate the opportunity of integrating microalgae-bacteria cultivation in side-stream digestate treatment processes, in view of generating bioproducts at the industrial scale, while guaranteeing the valorisation of digestate nutrients.

## Declaration of Competing Interest

The authors declare that they have no known competing financial interests or personal relationships that could have appeared to influence the work reported in this paper.

## Data availability

Data will be made available on request.

## Acknowledgments

This research was funded by European Union (Project: *BIO-METHAVERSE – Demonstrating and Connecting Production Innovations in the BIOMETHAne universe*, grant ID 101084200) and Regione Lombardia (Project: *PerFORM WATER 2030*). The authors would like to thank: Dr. Eng. D. Scaglione and Eng. R. di Cosmo (Gruppo CAP) for providing WWTP data and for the assistance on pilot plant operations, Eng. D. Basilico (SEAM Engineering) for the design and assistance on the pilot plant, and all the students involved in the monitoring of the pilot plant.

## References

[1] J.L. Campos, D. Valenzuela-Heredia, A. Pedrouso, A. Val del Río, M. Belmonte, A. Mosquera-Corral, Greenhouse Gases Emissions from Wastewater Treatment Plants: Minimization, Treatment, and Prevention, J. Chem. (2016, 2016,) e3796352.

[2] D. Rosso, L.E. Larson, M.K. Stenstrom, Aeration of Large-Scale Municipal Wastewater Treatment Plants: State of the Art, Water Sci. Technol. 57 (7) (2008) 973–978, https://doi.org/10.2166/wst.2008.218.

[3] A. Daverey, D. Pandey, P. Verma, S. Verma, V. Shah, K. Dutta, K. Arunachalam, Recent Advances in Energy Efficient Biological Treatment of Municipal Wastewater, Bioresour. Technol. Rep. 7 (2019), 100252, https://doi.org/10.1016/j.biteb.2019.100252.

[4] K. Li, Q. Liu, F. Fang, R. Luo, Q. Lu, W. Zhou, S. Huo, P. Cheng, J. Liu, M. Addy, P. Chen, D. Chen, R. Ruan, Microalgae-Based Wastewater Treatment for Nutrients Recovery: A Review, Bioresour. Technol. 291 (2019), 121934, https://doi.org/10.1016/j.biortech.2019.121934.

[5] N.G.A.I. Karya, N.P. van der Steen, P.N.L. Lens, Photo-Oxygenation to Support Nitrification in an Algal-Bacterial Consortium Treating Artificial Wastewater, Bioresour. Technol. 134 (2013) 244–250, https://doi.org/10.1016/j.biortech.2013.02.005.

[6] S. Rossi, E. Sforza, M. Pastore, M. Bellucci, F. Casagli, F. Marazzi, E. Ficara, Photo-Respirometry to Shed Light on Microalgae-Bacteria Consortia—a Review, Rev. Environ. Sci. Biotechnol. 19 (1) (2020) 43–72, https://doi.org/10.1007/s11157-020-09524-2.

[7] R.K. Goswami, S. Mehariya, P. Verma, R. Lavecchia, A. Zuorro, Microalgae-Based Biorefineries for Sustainable Resource Recovery from Wastewater, J. Water Process Eng. 40 (2021), 101747, https://doi.org/10.1016/j.jwpe.2020.101747.

[8] F.G.A. Fernández, A. Reis, R.H. Wijffels, M. Barbosa, V. Verdelho, B. Llamas, The Role of Microalgae in the Bioeconomy, New Biotechnol. 61 (2021) 99–107, https://doi.org/10.1016/j.nbt.2020.11.011.

[9] L. Gouveia, S. Graça, C. Sousa, L. Ambrosano, B. Ribeiro, E.P. Botrel, P.C. Neto, A. F. Ferreira, C.M. Silva, Microalgae Biomass Production Using Wastewater: Treatment and Costs: Scale-up Considerations, Algal Res. 16 (2016) 167–176, https://doi.org/10.1016/j.algal.2016.03.010.

[10] J.C.M. Pires, M.C.M. Alvim-Ferraz, F.G. Martins, M. Simões, Wastewater Treatment to Enhance the Economic Viability of Microalgae Culture, Environ. Sci. Pollut. Res. 20 (8) (2013) 5096–5105, https://doi.org/10.1007/s11356-013-1791-x.

[11] J. González-Camejo, J. Ferrer, A. Seco, R. Barat, Outdoor Microalgae-Based Urban Wastewater Treatment: Recent Advances, Applications, and Future Perspectives, WIREs Water 8 (3) (2021) e1518.

[12] Y. Wang, S.-H. Ho, C.-L. Cheng, W.-Q. Guo, D. Nagarajan, N.-Q. Ren, D.-J. Lee, J.-S. Chang, Perspectives on the Feasibility of Using Microalgae for Industrial Wastewater Treatment, Bioresour. Technol. 222 (2016) 485–497, https://doi.org/10.1016/j.biortech.2016.09.106.

[13] F. Marazzi, M. Bellucci, S. Rossi, R. Fornaroli, E. Ficara, V. Mezzanotte, Outdoor Pilot Trial Integrating a Sidestream Microalgae Process for the Treatment of Centrate under Non Optimal Climate Conditions, Algal Res. 39 (2019), 101430, https://doi.org/10.1016/j.algal.2019.101430.

[14] A. Pizzera, D. Scaglione, M. Bellucci, F. Marazzi, V. Mezzanotte, K. Parati, E. Ficara, Digestate Treatment with Algae-Bacteria Consortia: A Field Pilot-Scale Experimentation in a Sub-Optimal Climate Area, Bioresour. Technol. 274 (2019) 232–243, https://doi.org/10.1016/j.biortech.2018.11.067.

[15] M. Mantovani, F. Marazzi, R. Fornaroli, M. Bellucci, E. Ficara, V. Mezzanotte, Outdoor Pilot-Scale Raceway as a Microalgae-Bacteria Sidestream Treatment in a WWTP, Sci. Total Environ. 710 (2020), 135583, https://doi.org/10.1016/j.scitotenv.2019.135583.

[16] Casagli, F.; Rossi, S.; Steyer, J. P.; Bernard, O.; Ficara, E. Balancing Microalgae and Nitrifiers for Wastewater Treatment: Can Inorganic Carbon Limitation Cause an Environmental Threat? *Environ. Sci. Technol.* **2021**, acs.est.0c05264. 10.1021/acs.est.0c05264.

[17] M. Sulev, J. Ross, Conversion Factor between Global Solar Radiation and Photosynthetic Active Radiation. In *Short Rotation Willow Coppice for Renewable Energy and Improved Environment*; Swedish University of Agricultural Sciences, 1995; pp 115–121.

[18] A. Parsy, L. Bidoire, M. Saadouni, M. Bahuaud, T. Elan, F. Périé, C. Sambusiti, Impact of Seasonal Variations on Nannochloropsis Oculata Phototrophic Productivity in an Outdoor Pilot Scale Raceway, Algal Res. 58 (2021), 102375, https://doi.org/10.1016/j.algal.2021.102375.

[19] APHA, AWWA, WEF. *Standard Methods for the Examination of Water and Wastewater, 23rd Edition*; 2017.

[20] F. Casagli, G. Zuccaro, O. Bernard, J.-P. Steyer, E. Ficara, ALBA: A Comprehensive Growth Model to Optimize Algae-Bacteria Wastewater Treatment in Raceway Ponds, Water Res. 190 (2021), 116734, https://doi.org/10.1016/j.watres.2020.116734.

[21] S. Rossi, A. Pizzera, M. Bellucci, F. Marazzi, V. Mezzanotte, K. Parati, E. Ficara, Piggery Wastewater Treatment with Algae-Bacteria Consortia: Pilot-Scale Validation and Techno-Economic Evaluation at Farm Level, Bioresour. Technol. 351 (2022), 127051, https://doi.org/10.1016/j.biortech.2022.127051.

[22] J.B.K. Park, R.J. Craggs, A.N. Shilton, Wastewater Treatment High Rate Algal Ponds for Biofuel Production, Bioresour. Technol. 102 (1) (2011) 35–42, https://doi.org/10.1016/j.biortech.2010.06.158.

[23] A.C. Anthonisen, R.C. Loehr, T.B.S. Prakasam, E.G. Srinath, Inhibition of Nitrification by Ammonia and Nitrous Acid, J. Water Pollut. Control Fed. 48 (5) (1976) 835–852.

[24] S. Rossi, R. Díez-Montero, E. Rueda, F. Castillo Cascino, K. Parati, J. García, E. Ficara, Free Ammonia Inhibition in Microalgae and Cyanobacteria Grown in Wastewaters: Photo-Respirometric Evaluation and Modelling, Bioresour. Technol. 305 (2020), 123046, https://doi.org/10.1016/j.biortech.2020.123046.

[25] F. Javed, M. Aslam, N. Rashid, Z. Shamair, A.L. Khan, M. Yasin, T. Fazal, A. Hafeez, F. Rehman, M.S.U. Rehman, Z. Khan, J. Iqbal, A.A. Bazmi, Microalgae-Based Biofuels, Resource Recovery and Wastewater Treatment: A Pathway towards Sustainable Biorefinery, Fuel 255 (2019), 115826, https://doi.org/10.1016/j.fuel.2019.115826.

[26] T. Mathimani, A. Pugazhendhi, Utilization of Algae for Biofuel, Bio-Products and Bio-Remediation, Biocatal. Agric. Biotechnol. 17 (2019) 326–330, https://doi.org/10.1016/j.bcab.2018.12.007.

[27] I. Pancha, K. Chokshi, S. Mishra, Industrial Wastewater-Based Microalgal Biorefinery: A Dual Strategy to Remediate Waste and Produce Microalgal Bioproducts. In *Application of Microalgae in Wastewater Treatment: Volume 2: Biorefinery Approaches of Wastewater Treatment*; Gupta, S. K., Bux, F., Eds.; Springer

International Publishing: Cham, 2019; pp 173–193. 10.1007/978-3-030-13909-4_8.
[28] B.A. Pessi, E. Pruvost, A. Talec, A. Sciandra, O. Bernard, Does Temperature Shift Justify Microalgae Production under Greenhouse? Algal Res. 61 (2022), 102579 https://doi.org/10.1016/j.algal.2021.102579.
[29] R. Davis, J. Markham, C. Kinchin, N. Grundl, E.C.D. Tan, D. Humbird, Process Design and Economics for the Production of Algal Biomass: Algal Biomass Production in Open Pond Systems and Processing Through Dewatering for Downstream Conversion; NREL/TP–5100-64772, 1239893; U.S. Department of Energy Office of Energy Efficiency & Renewable, Energy (2016), https://doi.org/10.2172/1239893.
[30] A. Ortiz, M.J. García-Galán, J. García, R. Díez-Montero, Optimization and Operation of a Demonstrative Full Scale Microalgae Harvesting Unit Based on Coagulation, Flocculation and Sedimentation, Sep. Purif. Technol. 259 (2021), 118171, https://doi.org/10.1016/j.seppur.2020.118171.
[31] S. Rossi, S. Visigalli, F. Castillo Cascino, M. Mantovani, V. Mezzanotte, K. Parati, R. Canziani, A. Turolla, E. Ficara, Metal-Based Flocculation to Harvest Microalgae: A Look beyond Separation Efficiency, Sci. Total Environ. 799 (2021), 149395, https://doi.org/10.1016/j.scitotenv.2021.149395.
[32] J. Ruiz, G. Olivieri, J.de Vree, R. Bosma, P. Willems, J.H. Reith, M.H.M. Eppink, D. M.M. Kleinegris, R.H. Wijffels, M.J. Barbosa, Towards Industrial Products from Microalgae, Energy Environ. Sci. 9 (10) (2016) 3036–3043, https://doi.org/10.1039/C6EE01493C.
[33] J. Ruiz, R.H. Wijffels, M. Dominguez, M.J. Barbosa, Heterotrophic vs Autotrophic Production of Microalgae: Bringing Some Light into the Everlasting Cost Controversy, Algal Res. 64 (2022), 102698, https://doi.org/10.1016/j.algal.2022.102698.
[34] Eurostat. *Agricultural land prices by region*. https://appsso.eurostat.ec.europa.eu/nui/submitViewTableAction.do (accessed 2022-06-06).
[35] Y. Chisti, Biodiesel from Microalgae, Biotechnol. Adv. 25 (3) (2007) 294–306, https://doi.org/10.1016/j.biotechadv.2007.02.001.
[36] N.C. Boelee, H. Temmink, M. Janssen, C.J.N. Buisman, R.H. Wijffels, Scenario Analysis of Nutrient Removal from Municipal Wastewater by Microalgal Biofilms, Water 4 (2) (2012) 460–473, https://doi.org/10.3390/w4020460.
[37] Rada-Ariza, A. M.; Alfonso-Martínez, A.; Leshem, U.; Lopez-Vazquez, C. M.; Van der Steer, N. P.; Lens, P. N. L. Nitrification in Pilot-Scale High Rate Algae Ponds Operated as Sequencing Batch Photo-Bioreactors for Anaerobically Treated Domestic Wastewater. **2016**.
[38] F.G. Acién, J.M. Fernández, J.J. Magán, E. Molina, Production Cost of a Real Microalgae Production Plant and Strategies to Reduce It, Biotechnol. Adv. 30 (6) (2012) 1344–1353, https://doi.org/10.1016/j.biotechadv.2012.02.005.
[39] D.S. Remer, L.H. Chai, Process Equipment, Cost Scale-Up, *Encycl. Chem. Process. Des.* 43 (1993) 306–317.
[40] F. Fasaei, J.H. Bitter, P.M. Slegers, A.J.B. van Boxtel, Techno-Economic Evaluation of Microalgae Harvesting and Dewatering Systems, Algal Res. 31 (2018) 347–362, https://doi.org/10.1016/j.algal.2017.11.038.
[41] B. Wett, Development and Implementation of a Robust Deammonification Process, Water Sci. Technol. 56 (7) (2007) 81–88, https://doi.org/10.2166/wst.2007.611.
[42] A.L. Gonçalves, M.C.M. Alvim-Ferraz, F.G. Martins, M. Simões, J.C.M. Pires, Integration of Microalgae-Based Bioenergy Production into a Petrochemical Complex: Techno-Economic Assessment, Energies 9 (4) (2016) 224, https://doi.org/10.3390/en9040224.
[43] ember-climate.org. *EU Carbon Price Tracker*. Ember. https://ember-climate.org/data/data-tools/carbon-price-viewer/ (accessed 2022-07-29).
[44] Eurostat. *Harmonised Indices of Consumer Prices (HICP)*. https://ec.europa.eu/eurostat/web/hicp/data/database (accessed 2022-08-07).
[45] N. Abdel-Raouf, A.A. Al-Homaidan, I.B.M. Ibraheem, Microalgae and Wastewater Treatment, Saudi J. Biol. Sci. 19 (3) (2012) 257–275, https://doi.org/10.1016/j.sjbs.2012.04.005.
[46] S. Barreiro-Vescovo, E. Barbera, A. Bertucco, E. Sforza, Integration of Microalgae Cultivation in a Biogas Production Process from Organic Municipal Solid Waste: From Laboratory to Pilot Scale, ChemEngineering 4 (2) (2020) 25, https://doi.org/10.3390/chemengineering4020025.
[47] N.-H. Norsker, M.J. Barbosa, M.H. Vermuë, R.H. Wijffels, Microalgal Production - A Close Look at the Economics, Biotechnol. Adv. 29 (1) (2011) 24–27, https://doi.org/10.1016/j.biotechadv.2010.08.005.
[48] J.B.K. Park, R.J. Craggs, Nutrient Removal in Wastewater Treatment High Rate Algal Ponds with Carbon Dioxide Addition, Water Sci. Technol. 63 (8) (2011) 1758–1764, https://doi.org/10.2166/wst.2011.114.
[49] M.L. Serejo, E. Posadas, M.A. Boncz, S. Blanco, P. García-Encina, R. Muñoz, Influence of Biogas Flow Rate on Biomass Composition During the Optimization of Biogas Upgrading in Microalgal-Bacterial Processes, Environ. Sci. Technol. 49 (5) (2015) 3228–3236, https://doi.org/10.1021/es5056116.
[50] M. del Morales-Amaral, M., Gómez-Serrano, C., Acién, F. G., Fernández-Sevilla, J. M., Molina-Grima, E. Outdoor Production of Scenedesmus Sp. in Thin-Layer and Raceway Reactors Using Centrate from Anaerobic Digestion as the Sole Nutrient Source, Algal Res. 12, 2015 99-108 10.1016/j.algal.2015.08.020.
[51] E. Posadas, D. Marín, S. Blanco, R. Lebrero, R. Muñoz, Simultaneous Biogas Upgrading and Centrate Treatment in an Outdoors Pilot Scale High Rate Algal Pond, Bioresour. Technol. 232 (2017) 133–141, https://doi.org/10.1016/j.biortech.2017.01.071.
[52] A. Morillas-España, A. Sánchez-Zurano, C. Gómez-Serrano, M. Ciardi, G. Acién, E. Clagnan, F. Adani, T. Lafarga, Potential of the Cyanobacteria Anabaena Sp. and Dolichospermum Sp. for Being Produced Using Wastewater or Pig Slurry: Validation Using Pilot-Scale Raceway Reactors, Algal Res. 60 (2021), 102517, https://doi.org/10.1016/j.algal.2021.102517.
[53] I. de Godos, S. Blanco, P.A. García-Encina, E. Becares, R. Muñoz, Influence of Flue Gas Sparging on the Performance of High Rate Algae Ponds Treating Agro-Industrial Wastewaters, J. Hazard. Mater. 179 (1) (2010) 1049–1054, https://doi.org/10.1016/j.jhazmat.2010.03.112.
[54] Z. Arbib, I. de Godos, J. Ruiz, J.A. Perales, Optimization of Pilot High Rate Algal Ponds for Simultaneous Nutrient Removal and Lipids Production, Sci. Total Environ. 589 (2017) 66–72, https://doi.org/10.1016/j.scitotenv.2017.02.206.
[55] A.F. Torres-Franco, C.C. Figueredo, L. Barros, B. Gücker, I.G. Boëchat, R. Muñoz, C. R. Mota, Assessment of a Deep, LED-Enhanced High-Rate Algal Pond for the Treatment of Digestate, Algal Res. 59 (2021), 102444, https://doi.org/10.1016/j.algal.2021.102444.
[56] A. Bani, K. Parati, A. Pozzi, C. Previtali, G. Bongioni, A. Pizzera, E. Ficara, M. Bellucci, Comparison of the Performance and Microbial Community Structure of Two Outdoor Pilot-Scale Photobioreactors Treating Digestate, Microorganisms 8 (11) (2020) 1754, https://doi.org/10.3390/microorganisms8111754.
[57] T. Bongiorno, L. Foglio, L. Proietti, M. Vasconi, A. Lopez, A. Pizzera, D. Carminati, A. Tava, A.J. Vizcaíno, F.J. Alarcón, E. Ficara, K. Parati, Microalgae from Biorefinery as Potential Protein Source for Siberian Sturgeon (A. Baerii) Aquafeed, Sustainability 12 (21) (2020) 8779, https://doi.org/10.3390/su12218779.
[58] M. Raeisossadati, A. Vadiveloo, P.A. Bahri, D. Parlevliet, N.R. Moheimani, Treating Anaerobically Digested Piggery Effluent (ADPE) Using Microalgae in Thin Layer Reactor and Raceway Pond, J. Appl. Phycol. 31 (4) (2019) 2311–2319, https://doi.org/10.1007/s10811-019-01760-6.
[59] C. Ledda, G.I. Romero Villegas, F. Adani, F.G. Acién Fernández, E. Molina Grima, Utilization of Centrate from Wastewater Treatment for the Outdoor Production of Nannochloropsis Gaditana Biomass at Pilot-Scale, Algal Res. 12 (2015) 17–25, https://doi.org/10.1016/j.algal.2015.08.002.
[60] D.L. Sutherland, J. Park, S. Heubeck, P.J. Ralph, R.J. Craggs, Size Matters – Microalgae Production and Nutrient Removal in Wastewater Treatment High Rate Algal Ponds of Three Different Sizes, Algal Res. 45 (2020), 101734, https://doi.org/10.1016/j.algal.2019.101734.
[61] G.I. Romero-Villegas, M. Fiamengo, F.G. Acién-Fernández, E. Molina-Grima, Utilization of Centrate for the Outdoor Production of Marine Microalgae at the Pilot-Scale in Raceway Photobioreactors, J. Environ. Manage. 228 (2018) 506–516, https://doi.org/10.1016/j.jenvman.2018.08.020.
[62] A. Jebali, F.G. Acién, E. Rodriguez Barradas, E.J. Olguín, S. Sayadi, E. Molina Grima, Pilot-Scale Outdoor Production of Scenedesmus Sp. in Raceways Using Flue Gases and Centrate from Anaerobic Digestion as the Sole Culture Medium, Bioresour. Technol. 262 (2018) 1–8, https://doi.org/10.1016/j.biortech.2018.04.057.
[63] R. Jiang, L. Qin, S. Feng, D. Huang, Z. Wang, S. Zhu, The Joint Effect of Ammonium and PH on the Growth of Chlorella Vulgaris and Ammonium Removal in Artificial Liquid Digestate, Bioresour. Technol. 325 (2021), 124690, https://doi.org/10.1016/j.biortech.2021.124690.
[64] D. Scaglione, G. Tornotti, A. Teli, L. Lorenzoni, E. Ficara, R. Canziani, F. Malpei, Nitrification Denitrification via Nitrite in a Pilot-Scale SBR Treating the Liquid Fraction of Co-Digested Piggery/Poultry Manure and Agro-Wastes, Chem. Eng. J. 228 (2013) 935–943, https://doi.org/10.1016/j.cej.2013.05.075.
[65] F. Zhang, H. Yang, J. Wang, Z. Liu, Q. Guan, Effect of Free Ammonia Inhibition on NOB Activity in High Nitrifying Performance of Sludge, RSC Adv. 8 (56) (2018) 31987–31995, https://doi.org/10.1039/C8RA06198J.
[66] S. Park, W. Bae, Modeling Kinetics of Ammonium Oxidation and Nitrite Oxidation under Simultaneous Inhibition by Free Ammonia and Free Nitrous Acid, Process Biochem. 44 (6) (2009) 631–640, https://doi.org/10.1016/j.procbio.2009.02.002.
[67] A. Sánchez-Zurano, S. Rossi, J.M. Fernández-Sevilla, G. Acién-Fernández, E. Molina-Grima, E. Ficara, Respirometric Assessment of Bacterial Kinetics in Algae-Bacteria and Activated Sludge Processes, Bioresour. Technol. 352 (2022), 127116, https://doi.org/10.1016/j.biortech.2022.127116.
[68] V. Andreotti, A. Solimeno, S. Rossi, E. Ficara, F. Marazzi, V. Mezzanotte, J. García, Bioremediation of Aquaculture Wastewater with the Microalgae Tetraselmis Suecica: Semi-Continuous Experiments, Simulation and Photo-Respirometric Tests, Sci. Total Environ. 738 (2020), 139859, https://doi.org/10.1016/j.scitotenv.2020.139859.
[69] Davis, R.; Fishman, D.; Frank, E. D.; Wigmosta, M. S.; Aden, A.; Coleman, A. M.; Pienkos, P. T.; Skaggs, R. J.; Venteris, E. R.; Wang, M. Q. *Renewable Diesel from Algal Lipids: An Integrated Baseline for Cost, Emissions, and Resource Potential from a Harmonized Model*; NREL/TP-5100-55431, ANL/ESD/12-4, 1044475; 2012; p NREL/TP-5100-55431, ANL/ESD/12-4, 1044475. 10.2172/1044475.
[70] J. Richardson, J.L. Outlaw, M. Allison, The Economics of Microalgae Oil, AgBioForum 13 (2010) 119–130.
[71] K. Pelendridou, M.K. Michailides, D.P. Zagklis, A.G. Tekerlekopoulou, C. A. Paraskeva, D.V. Vayenas, Treatment of Olive Mill Wastewater Using a Coagulation-Flocculation Process Either as a Single Step or as Post-Treatment after Aerobic Biological Treatment, J. Chem. Technol. Biotechnol. 89 (12) (2014) 1866–1874, https://doi.org/10.1002/jctb.4269.
[72] A. Al Ketife, F. Almomani, M. El-Naas, S. Judd, A Technoeconomic Assessment of Microalgal Culture Technology Implementation for Combined Wastewater Treatment and CO2 Mitigation in the Arabian Gulf, 2019 Process Saf. Environ Prot.
[73] S. Chaudry, Integrating Microalgae Cultivation with Wastewater Treatment: A Peek into Economics, Appl. Biochem. Biotechnol. 193 (10) (2021) 3395–3406, https://doi.org/10.1007/s12010-021-03612-x.
[74] J.-C. Lee, B. Lee, H.-W. Kim, B.-H. Jeon, H. Lim, Techno-Economic Analysis of Livestock Urine and Manure as a Microalgal Growth Medium, Waste Manag. 135 (2021) 276–286, https://doi.org/10.1016/j.wasman.2021.09.005.
[75] H. Leflay, K. Okurowska, J. Pandhal, S. Brown, Pathways to Economic Viability: A Pilot Scale and Techno-Economic Assessment for Algal Bioremediation of

Challenging Waste Streams, Environ. Sci. Water Res. Technol. 6 (12) (2020) 3400–3414, https://doi.org/10.1039/D0EW00700E.

[76] F.A. Ansari, B. Ravindran, S.K. Gupta, M. Nasr, I. Rawat, F. Bux, Techno-Economic Estimation of Wastewater Phycoremediation and Environmental Benefits Using Scenedesmus Obliquus Microalgae, J. Environ. Manage. 240 (2019) 293–302, https://doi.org/10.1016/j.jenvman.2019.03.123.

[77] E. Moral Pajares, L. Gallego Valero, I.M. Román Sánchez, Cost of Urban Wastewater Treatment and Ecotaxes: Evidence from Municipalities in Southern Europe, Water 11 (3) (2019) 423, https://doi.org/10.3390/w11030423.

[78] G. Rodriguez-Garcia, M. Molinos-Senante, A. Hospido, F. Hernández-Sancho, M. T. Moreira, G. Feijoo, Environmental and Economic Profile of Six Typologies of Wastewater Treatment Plants, Water Res. 45 (18) (2011) 5997–6010, https://doi.org/10.1016/j.watres.2011.08.053.

[79] I. Ruiz-Rosa, F.J. García-Rodríguez, J. Mendoza-Jiménez, Development and Application of a Cost Management Model for Wastewater Treatment and Reuse Processes, J. Clean. Prod. 113 (2016) 299–310, https://doi.org/10.1016/j.jclepro.2015.12.044.

[80] Y. Lin, M. Guo, N. Shah, D.C. Stuckey, Economic and Environmental Evaluation of Nitrogen Removal and Recovery Methods from Wastewater, Bioresour. Technol. 215 (2016) 227–238, https://doi.org/10.1016/j.biortech.2016.03.064.

[81] H.W.H. Menkveld, E. Broeders, Recovery of Ammonia from Digestate as Fertilizer, Water Pract. Technol. 13 (2) (2018) 382–387, https://doi.org/10.2166/wpt.2018.049.

[82] Y.I.D. Yousif, E.Sh. Mohamed, A.S. El-Gendy, Using chlorella vulgaris for nutrient removal from hydroponic wastewater: Experimental investigation and economic assessment, Water Sci. Technol. 2022157 (2022), https://doi.org/10.2166/wst.2022.157.

[83] A.K. Kumar, S. Sharma, G. Dixit, E. Shah, A. Patel, Techno-economic analysis of microalgae production with simultaneous dairy effluent treatment using a pilot-scale High Volume V-shape pond system, Renew. Energ. 145 (2020) 1620–1632, https://doi.org/10.1016/j.renene.2019.07.087.